Science Advances
AAAS

Supplementary Materials for

Deep brain stimulation of the thalamus restores signatures of consciousness in a nonhuman primate model

Jordy Tasserie, Lynn Uhrig, Jacobo D. Sitt, Dragana Manasova, Morgan Dupont, Stanislas Dehaene, Béchir Jarraya*

*Corresponding author. Email: bechir.jarraya@cea.fr

Published 18 March 2022, *Sci. Adv.* **8**, eabl5547 (2022)
DOI: 10.1126/sciadv.abl5547

This PDF file includes:

Supplementary Text

-Extended Materials and Methods

Deep brain stimulation (DBS) methodology

Surgery using neuro-navigation

We implanted a four-lead (0, 1, 2, 3) MRI-compatible clinical DBS electrode (Medtronic 3389, USA) in two macaques (monkey N and T) with the ultimate goal of performing simultaneous DBS-fMRI acquisitions. Electrode leads were 1.5 mm long and spaced by 0.5 mm. The external diameter was 1.27 mm. We targeted the right centro-median thalamus (CM) and performed aseptic stereotaxic surgery under general anesthesia using a neuro-navigation system (BrainSight, Rogue, Canada) guided by anatomical 3T MRI (Prisma Fit, Siemens, Germany) (MPRAGE, T1 weighted, repetition time TR = 2200ms; inversion time TI=900ms, 0.80mm isotropic voxel size, sagittal orientation, mono-channel 1Tx-1Rx circular surface coil of 12.5 cm diameter). The head of the monkey was placed in a stereotaxic frame and maintained with ears and ocular bars. All devices were built in plastic and MR compatible materials. Gadolinium fiducials were placed on the frame, as well as on the macaque skull and the temporary headpost that held additional fiducials. These landmarks, recognized by the neuro-navigation system, were put all around the skull in a non-coplanar manner. Pre-operative MRI images aimed at defining the target and trajectory. We assessed the target location and trajectory according to the MNI macaque brain coordinates (x, y, z) and Paxinos Atlas reference space (L, B, S). We confirmed the contact spot following three other approaches: i) anterior-posterior commissure (AC-PC) system; ii) distance to different anatomical area landmarks such as the right caudate nucleus and iii) Saleem Atlas. Lead placement trajectory was simulated with the neuro-navigation module prior to surgery.

We drilled craniotomy, positioned a plastic cannula to guide the DBS electrode and fixed an anchoring device system (Stim-lock, Medtronic, USA) covering the craniotomy. This element aimed at stabilizing and blocking the lead extremity to avoid lead migration. Per-operative MRI were acquired to control convergence between the theoretical and the practical implantation spot (effective target reached during surgery versus desired planned location). The extracranial part of the lead was

protected with a plastic MR compatible chamber that was home-made by 3D-printing and was fixed to the skull with screws and dental acrylic.

Verification of the DBS settings and underlying behavioral responses

To ensure efficiency across experiments, impedances between leads and through electrode to an external reference were first measured outside the MRI environment with the DBS programmer device provided by the manufacturer (8840 N'Vision, Activa Clinician DBS Programmer, Medtronic, USA). Ultimately, we used an oscilloscope (Wave Runner 44XI, LeCroy, USA) to check the electrical current delivered to each lead at the beginning and at the end of each experimental session. The stimulation also generated an artifact on the EEG signal, which provided a final benchmark during the fMRI acquisitions.

Behavioral responses (see behavioral assessment section) to electrical thalamic stimulation were assessed in each animal outside the scanner at least 20 days after the DBS implantation. We empirically explored different voltage amplitudes and pulse widths while keeping a monopolar stimulation at a frequency of 130Hz, applied successively to each of the four DBS contacts. The DBS lead targeted the centro-median thalamus. On the target contact (centered in CM), we determined the voltage level for high central thalamic (CT) DBS as the voltage just above the threshold at which a significant behavioral response was observed. Low CT-DBS corresponded to a lower current delivery below the voltage level that led to an arousal pattern. For comparison and reproducibility purposes, we kept the exact same DBS settings for the control stimulation site (ventro-lateral thalamus (VL) DBS).

fMRI statistical analysis

Block-design fMRI analysis

We generated plots by extracting the activations responses to high CT-DBS with the hemodynamic function in frontal (area 6V; 9/46; 8A), parietal (ventral intraparietal VIP, parietal area PFG), cingulate (anterior ACC: posterior PCC) and temporal cortex (temporo-parieto-occipital area TPO). Activity profiles were plotted as percentage of signal changes across time.

Resting-state fMRI analysis

For the static resting state, we calculated for each experimental condition and sessions the average of positive and negative Z-values and performed a Student t-test with the null hypothesis of zero correlation to test for statistical significance of connectivity between the different experimental conditions.

We computed the static functional correlations by estimating for each experimental condition (noted *e*) for the awake state, anesthesia, low CT-DBS, high CT-DBS, low VL-DBS and high VL-DBS and acquired run (noted *r*) the covariance matrix $C_{e,r}$. This value was obtained by extracting and averaging across all runs *r* the time series of all voxels included in each selected anatomical ROI. We referred as static functional correlation or stationary functional connectivity the entry matrix $C_{e,r}$ (i,j) where each cell represented the mean strength of the functional correlation between the i-j pair. For each covariance matrix, a Fisher transformation was applied to calculate the Z-score. The Z-score matrices were averaged across runs to obtain one matrix per experimental condition. To assess statistical significance, Student t-test at the threshold p value<0.0001 and a false discovery rate correction were applied on the correlations of all pairs of brain regions.

Dynamic resting state fMRI analysis

Covariance values between all ROIs were included ([82×(82−1)]/2=3,321 features per matrix). $Z_{c,s,w}$ matrices were subsampled along the time dimension (*w*) before clustering. The resulting centroids or median clusters (BS_n with n=1–7; each BS_n is sized 82×82) were then used to initialize a clustering of all data, obtaining a matrix of brain states $B_{c,s,w,}$ which, for a given arousal condition c and session s, is a vector of length 464, valued 1–7, because each matrix in $Z_{s,p,w}$ is assigned a BS_n.

The similarity score was computed from the correlation coefficient between the vectorized structural matrix and each vectorized brain state from the clustering analysis. All brain states were ordered in ascending order of similarity to the structure using the similarity score. To quantify the relation between the probability of occurrence of a BS and the similarity score, for each arousal condition, a regression analysis was done, to quantify the beta value (β), the R^2 and a P value. The differences in BS composition across arousal states was evaluated through a fixed-effects ANOVA, with mean rank similarity, that is, the result of averaging each BS time series, valued from 1 to 7, as a dependent

variable and the vigilance condition as the in-dependent variable. A fixed-effects ANOVA was run to quantify the effect of sedation on the probability of brain state 7. For this, we followed the same procedure, but the mean rank similarity was calculated considering only BS 7 (window *w* valued at 1; any other state window *w* valued at 0).

To explore specifically the fluctuations of intervoxel correlation within nodes of the "macaque global neuronal worskspace" and sensori-motor areas (anterior cingulate cortex, ACC; dorsolateral prefrontal cortex, PFCdl; frontal eye fields, FEF; dorsolateral premotor cortex, PMCdl; primary somatosensory cortex, S1; primary motor cortex, M1; intraparietal cortex, Pcip; primary auditory cortex, A1; inferior temporal cortex, TCi; visual area 1, V1 and posterior cingulate cortex, PCC), we extracted the values from the whole brain matrices and applied a one-way analysis of variance (ANOVA). FC across the brain states were highlighted by displaying Z-score in inter-region matrices.

Event-related task fMRI analysis

We generated plots by obtaining the β-weight of SPM regressions of individual macaque data with the hemodynamic functions of the appropriate stimulus categories and then plotted the mean and SE of these β-weights. These values estimate, in percentages of the whole-brain fMRI signal, the size of the fMRI activation relative to the implicit rest baseline that divides trials.

The first level analyses consisted in the convolution of the stimulus categories with the MION canonical hemodynamic response function (HRF) and its time derivative. We also added motion regressors and heart rate as variables of non-interest to the event-related regressors. Activation time series of all the fMRI voxels were computed for each fMRI run and signal change expressed in T-score maps for the different stimulus categories relative to rest periods. Global standard trials that immediately followed a global deviant trial were excluded.

-Extended Results

<u>Thalamic DBS effects on resting-state networks in anesthetized macaques</u>

Static Functional Correlations (Figure 4, S6)

To test for statistical significance of connectivity between brain regions in different experimental

conditions, Student t-tests were performed with the null hypothesis of zero correlation. We calculated for each experimental condition *c* and sessions the average of positive and negative Z values of $Z_{c,s}$.

The average positive Z-value was 0.43+/-2.9e-4 in the awake state, 0.22+/-2.6e-4 under anesthesia, 0.27+/-2.5e-4 during low CT-DBS, 0.39+/-2.8e-4 during high CT-DBS, 0.28+/-3.1e-4 during low VL-DBS and 0.19+/-2.4e-4 during high VL-DBS *(Figure 4A)*. Positive Z-values were significantly different under anesthesia and high CT-DBS ($p < 0.001$, FDR corrected *(Figure 4A)*. The average negative Z-value was 0.24+/-4.2e-4 in the awake state, 0.09+/-1.7e-4 under anesthesia, 0.12+/-2.7-4 during low CT-DBS, 0.11+/-3.2e-4 during high CT-DBS, 0.08+/-2.7e-4 during low VL-DBS and 0.08+/-2.2e-4 during high VL-DBS *(Figure 4A)*. Negative Z-values were significantly different under anesthesia and high CT-DBS ($p < 0.001$, FDR corrected) *(Figure 4A)*. In the awake state, the frontal cortex (areas 9/46, 8A, 6V and M1), parietal cortex (parietal area PFG and ventral intraparietal area), anterior and posterior cingulate cortices, temporal cortex (area A1) and occipital cortex (area V1) were strongly correlated to each other *(left column, Figure 4B)*.

Dynamic Functional Correlations (Figure 5, S7-S8, Table S4)

We applied k-means to the whole acquired dataset (including all experimental conditions) to cluster brain states *(Figure S7)*. We also applied k-means to two data subsets, subset CT and subset VL, to specifically characterize the effects of CT-DBS and VL-DBS respectively. Subset CT included data from awake, anesthesia and anesthesia + high CT-DBS conditions *(Figure 5A-C)*. Subset VL included data from awake, anesthesia and anesthesia + high VL-DBS conditions *(Figure 5D-E)*.

-Clustering subset CT (data from awake, anesthesia and anesthesia + high CT-DBS conditions) (Figure 5A-C)

In the awake state, all 7 brain states were represented with a similar probability of occurrence ($\beta=0.45$; $R^2=0.22$; $p=0.28$). During anesthesia, state 7 (with the highest function-structure similarity) was dominant and state 1 (with the lowest function-structure similarity) never occurred ($\beta=1.91$; $R^2=0.67$; $p=0.02$). Under high CT-DBS, consistent with partial recovery of consciousness, the probability of occurrence of state 7 decreased in favor of all the other brain states, especially state 2 and 3 ($\beta=0.64$; $R^2=0.28$; $p=0.22$). We computed the slope of the linear relation between structural and functional

correlations for each recording session and compared the slope distributions in the awake, anesthesia and DBS conditions. Awake and high CT-DBS slopes were significantly lower than the anesthesia slopes, indicating that a greater diversity of states were explored in the wake state (awake versus anesthesia: t-test, p=6e-5 and BF10=338, high CT-DBS versus anesthesia: t-test, p=0.001 and BF10=23). Importantly no differences were observed between awake and high CT-DBS slopes (t-test, p=0.42, BF01=3.28) *(Figure 5A-B, Table S6)*. In the awake state, the mean rank of brain states was 4 (4.38±1.28), for anesthesia, the mean rank was 6 (5.70±1.40) and during high CT-DBS, the mean rank was 5 (4.55±1.17). This brain state distribution was significantly different (ANOVA; F(2;120)=12.52; p=1.15e-7). Also, the frequency of brain state 7 was moderate in the awake experiments (probability=0.24), high during anesthesia (probability=0.58) and low again during high CT-DBS (probability=0.26; p<0.0001) *(Figure 5B)*. The probability of brain state 7 was higher in anesthesia compared to the awake state (t-test, p=1e-6, BF10=9063) and to high CT-DBS (t-test, p=1e-5, BF10=1017) which did not differ significantly (t-test, p=0.74, BF01=4.18). The mean similarity with the anatomical connectivity was also significantly different with 0.24 (±0.06) for the awake state, 0.31 (±0.07) for anesthesia and 0.25 (±0.06) for high CT-DBS (ANOVA; F(2,120)=14.75; p=1.87e-6). Anatomically, the functional brain states 1, 2 and 3, that were most characteristic of the awake, presented strong correlations within the "macaque GNW" prefrontal (dorsolateral prefrontal cortex, PFCdl; dorsolateral premotor cortex, PMCdl), parietal (intraparietal cortex, PCip) and cingulate nodes (anterior cingulate cortex, ACC; posterior cingulate cortex, PCCr), whereas state 7 displayed low or null Z-score values across the same entire cortical network *(Figure 5C)*. During high CT-DBS, the average duration of brain state 7 decreased compared to anesthesia (high CT-DBS versus anesthesia, p=2.48e-3; bootstrap analysis) and was similar to the awake state *(Figure S8)*.

- *Clustering subset VL (data from awake, anesthesia and anesthesia + high VL-DBS conditions) (Figure 5D-E)*

In the awake state, all seven brain states were present (β=0.16; R^2=0.02; p=0.74). Under anesthesia, brain state 7 was dominant (β=1.21; R^2=0.33; p=0.18), as under high VL-DBS (β=1.69; R^2=0.43; p=0.11) *(Figure 5F-G)*. We also computed the slope corresponding to each recording session and

compared the slope distributions in the awake, anesthesia and high VL-DBS conditions. Awake slopes were significantly lower compared to anesthesia and high VL-DBS slopes (awake versus anesthesia: t-test, p=0.0007 and BF10=39, awake versus high CT-DBS: t-test, p=1e-8 and BF10=636824). The slopes under anesthesia were smaller than the high VL-DBS slopes (t-test, p=0.01, BF10=3.81).

For the awake state, the mean rank of brain states was 4 (4.41±0.93), under anesthesia, the mean rank was 6 (5.81±1.39) and under high VL-DBS, the mean rank was 6 (6.41±0.38). The brain state distribution was significantly different (ANOVA; F(2;102)=32.03; p=1.61e-11). Brain state 7 was balanced in the awake state (awake brain state 7 probability=0.19), dominant under anesthesia (anesthesia brain state 7 probability=0.60) and high VL-DBS (high VL-DBS brain state 7 probability=0.72; p<0.0001) (*Figure 5F*). The probability of state 7 was smaller in the awake state compared to anesthesia (t-test, p=10e-9, BF10=2e7) and compared to high VL-DBS (t-test, p=10e-17, BF10=1e15). However, we found no evidence for a difference nor a similarity between anesthesia and high VL-DBS (t-test, p=0.15, BF10=0.64, BF01=1.54).

Brain state 1 highlighted strong correlations to all the tested cortical areas. Brain state 7 presented weak Z-score values with prefrontal (PFCdl; PMCdl), parietal (PCip) and cingulate cortex (ACC; PCC) *(Figure 5C)*.

With high VL-DBS, the average duration of brain state 7 increased compared to the awake state (high VL-DBS v/s awake, p<0.0001, bootstrap analysis) and was similar to the anesthesia state *(Figure S8)*.

-Clustering the whole dataset (data from awake, anesthesia, low CT-DBS, high CT-DBS, low VL-DBS and high VL-DBS) (Figure S7)

The occurrence of brain states in the awake condition was equiprobable (β=0.05; R^2=0.003; p=0.91). Under anesthesia, this probability was shaped by the brain state 7 (β=1.87; R^2=0.59; p=0.04). For the DBS sessions, brain state probability of occurrence was partly dominated by brain state 7 in the low CT-DBS condition (β=1.09; R^2=0.49; p=0.08), balanced under high CT-DBS (β=0.28; R^2=0.059; p=0.6308), partly dominated by the brain state 7 during the low VL-DBS experiments (β=1.52; R^2=0.59; p=0.04) and dominated by brain state 7 in the high VL-DBS condition (β=2.57; R^2=0.73; p=0.01) *(Figure S7)*.

The mean rank was 4 in the awake state (3.81±1.05), 5 under anesthesia (5.37±1.34), 5 in the low CT-DBS condition (4.81±0.93), 4 in the high CT-DBS condition (4.14±1.03), 5 in the low VL-DBS condition (5.35±0.86) and 6 in the high VL-DBS condition (6.01±0.53). The brain state distribution was significantly different between structural and functional correlations (ANOVA; $F(5;193)=19.65$; $p=8.31e-16$) *(Figure S7)*. The probability of occurrence of brain state 7 was low in the awake state (0.20), and high under anesthesia (0.54). Crucially, even though anesthesia continued, low CT-DBS and high CT-DBS reduced this probability down to an aware level (respectively 0.37 and 0.23). The probability of state 7 also decreased with low VL-DBS (0.38) but returned to high (0.63, $p<0.001$) under high VL-DBS. The mean similarity with the anatomical connectivity was also significantly different with 0.26 (±0.04) for the awake state, 0.32 (±0.06) for anesthesia, 0.29 (±0.04) for low CT-DBS, 0.27 (±0.04) for high CT-DBS, 0.31 (±0.0.04) for low VL-DBS and 0.35 (±0.03) and for high VL-DBS (ANOVA; $F(5,193)=17.72$; $p=1.94e-14$). The average duration of brain state 7 significantly decreased with high CT-DBS compared to the anesthesia state ($p=1.61e-9$, bootstrap analysis) and was similar to the awake state. Low CT-DBS and low VL-DBS decreased the duration the brain state 7 compared to anesthesia (low CT-DBS v/s anesthesia, $p=6.72e-8$; low VL-DBS v/s anesthesia, $p=1.88e-7$, bootstrap analysis). Under high VL-DBS, duration of the brain state 7 was similar to the anesthesia state (high VL-DBS v/s anesthesia, not significant) *(Figure S7)*.

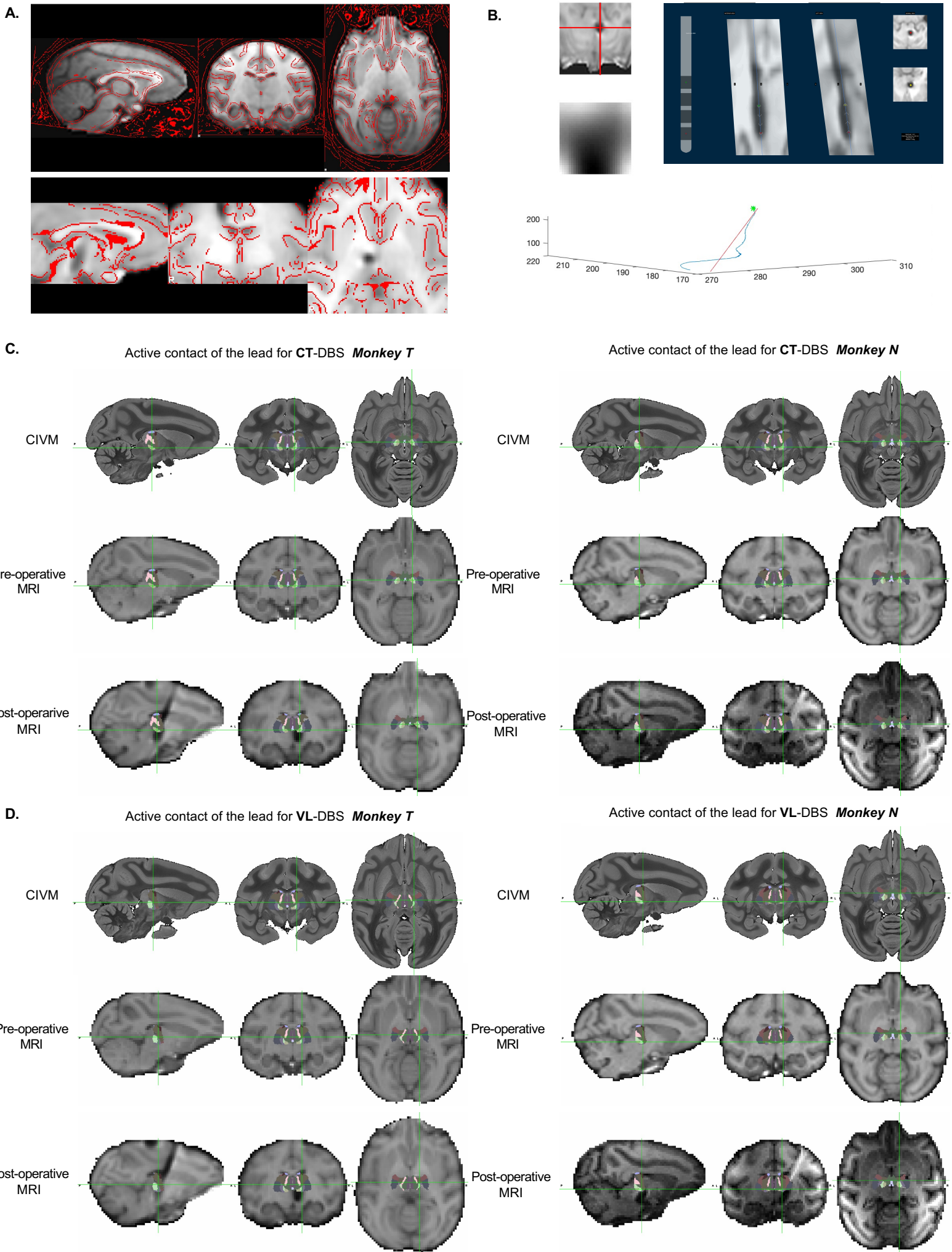

Figure S1: Localization of the DBS electrode contacts using the Lead-DBS macaque toolbox*(71)*. (A) Coregistration of the pre and post-operative MRI anatomical images (upper panel) and between MRI post-operative and MNI macaque brain atlas*(73)* (lower panel) for monkey T. (B) Pre-reconstruction of the electrode lead trajectory using the entry point on the anatomical MRI image and manual correction of electrode localization adjusting the most inferior (contact 0) and most superior (contact 3) DBS contacts according to the electrode artifact in two dimensional planes presented orthogonally. (C) Location of the centro-median (CM) DBS contact and (D) ventral-lateral thalamus (VL) DBS contact in monkey T (left column) and monkey N (right column) on the sagittal, coronal and axial plan. The target is displayed in the CIVM MRI atlas*(76)* (upper panel), pre-operative structural MRI (middle panel) and post-operative structural MRI (lower panel) warped in the MNI macaque space*(73)*.

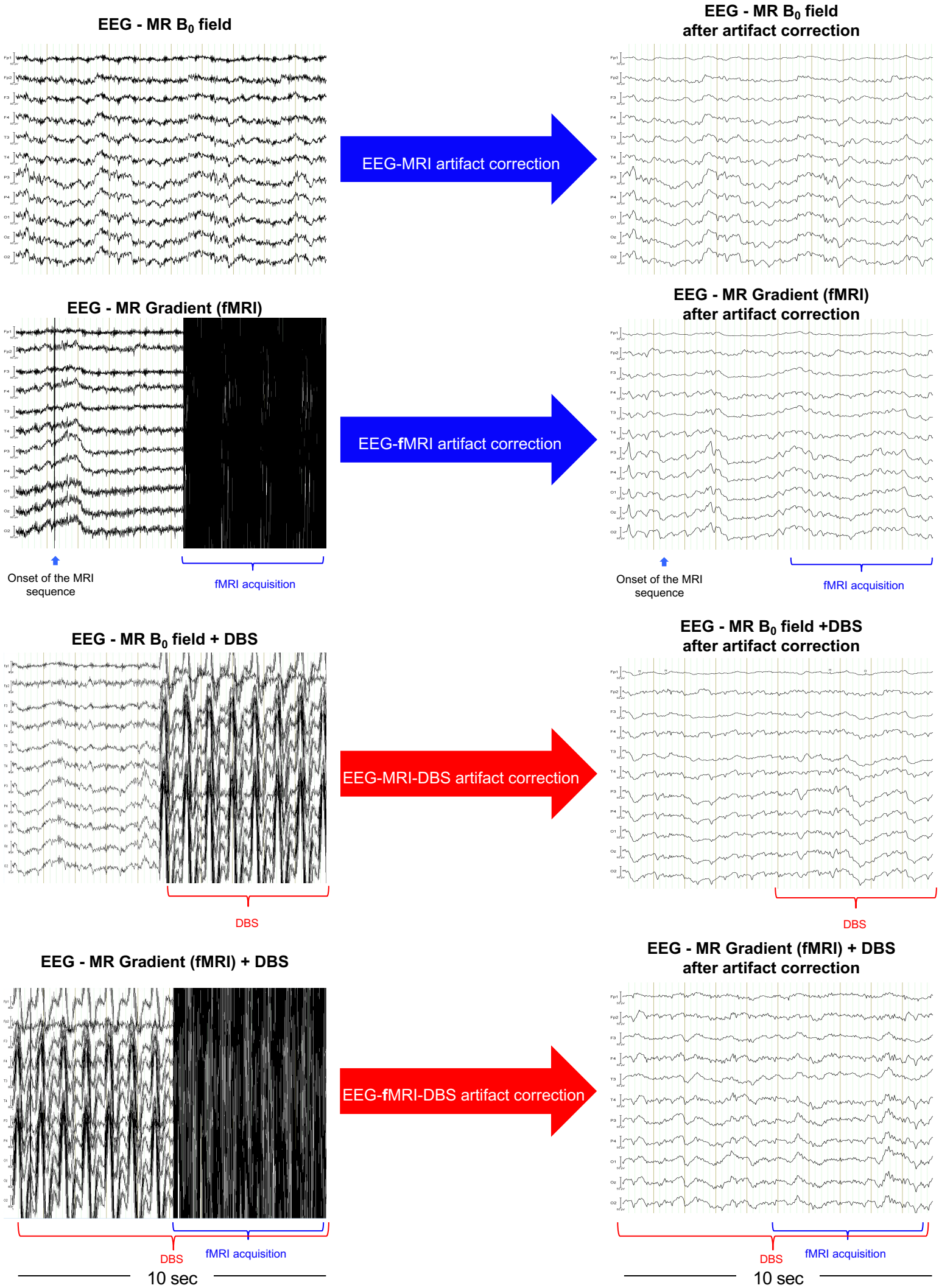

Figure S2: Suppression of EEG artifacts related to MR B_0 field, MR Gradients during fMRI acquisition and DBS. Examples of EEG recordings in anesthetized macaques inside a 3T MRI scanner without and with DBS of central thalamus (CT) thalamus at 3V.

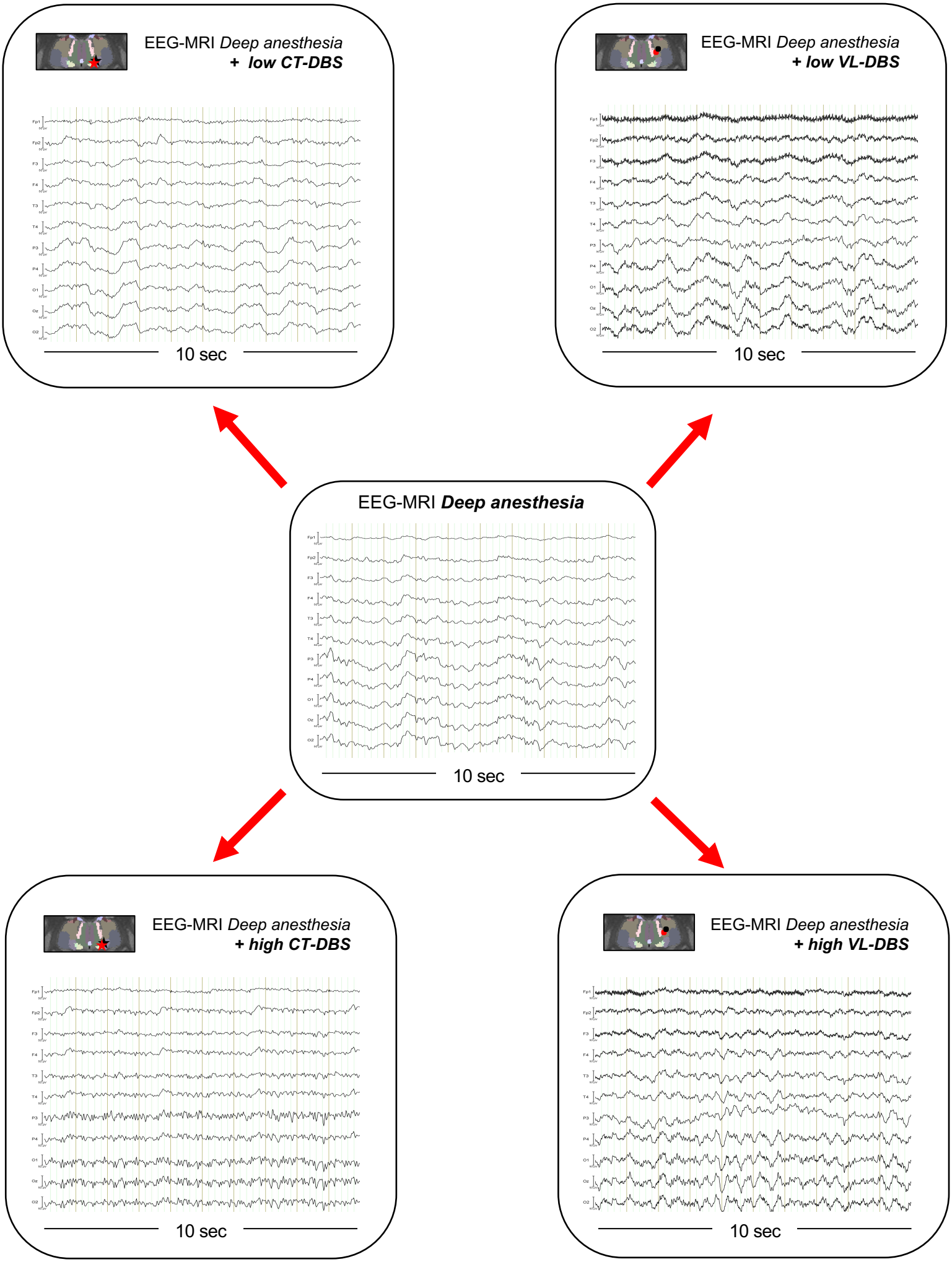

Figure S3: Effects of thalamic DBS on EEG. Examples of EEG recordings in anesthetized macaques inside a 3T MRI scanner with DBS of central thalamus (CT) or ventral-lateral thalamus (VL) at low or high voltages. The DBS-induced changes in cortical activity depends on the anatomical site of the active DBS lead contact and the intensity of the electrical stimulation.

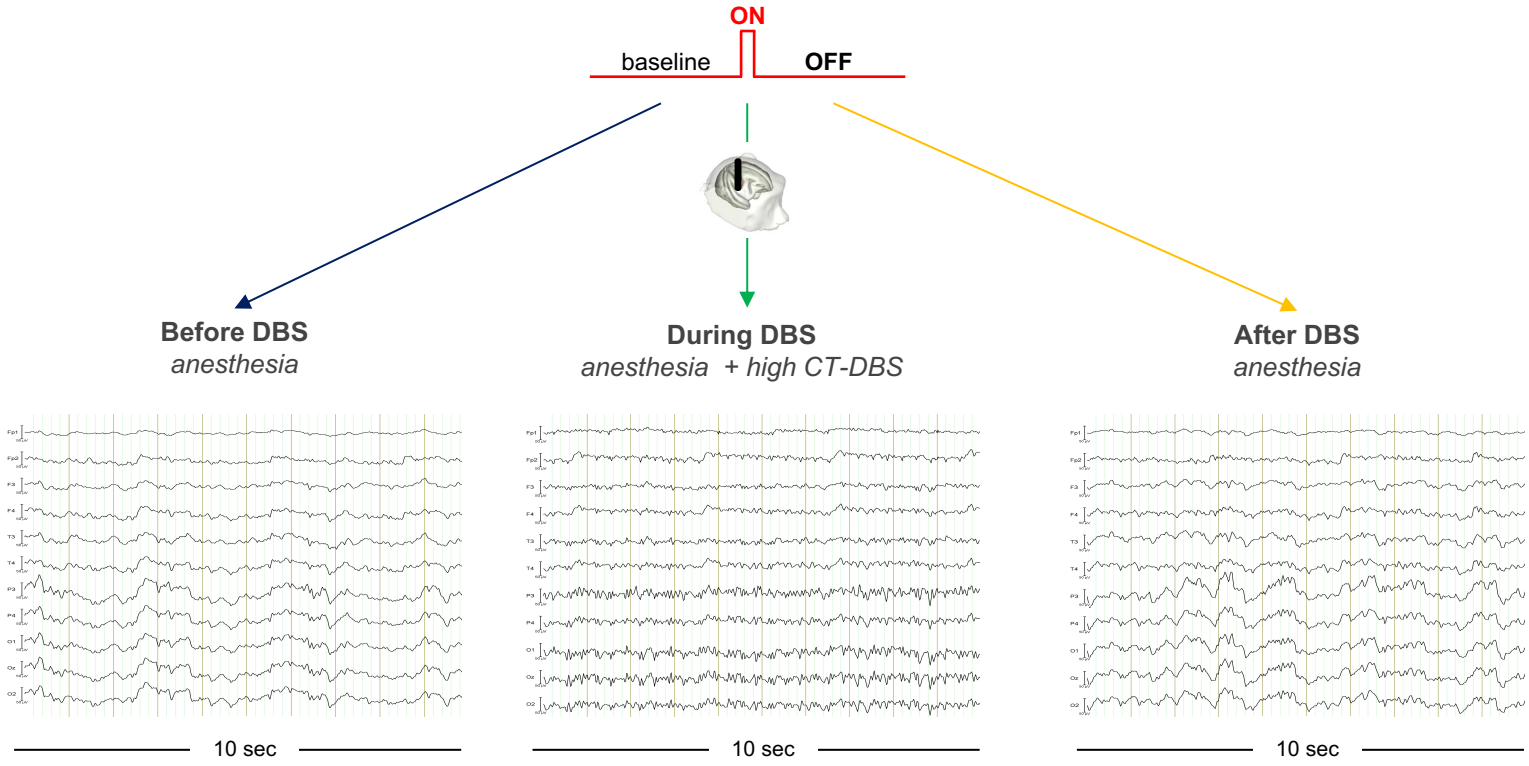

Figure S4: Cortical activity dynamic during and immediately after DBS

Examples of EEG recordings in anesthetized macaques inside a 3T MRI scanner before, during and after DBS of central thalamus (CT) at high voltage.

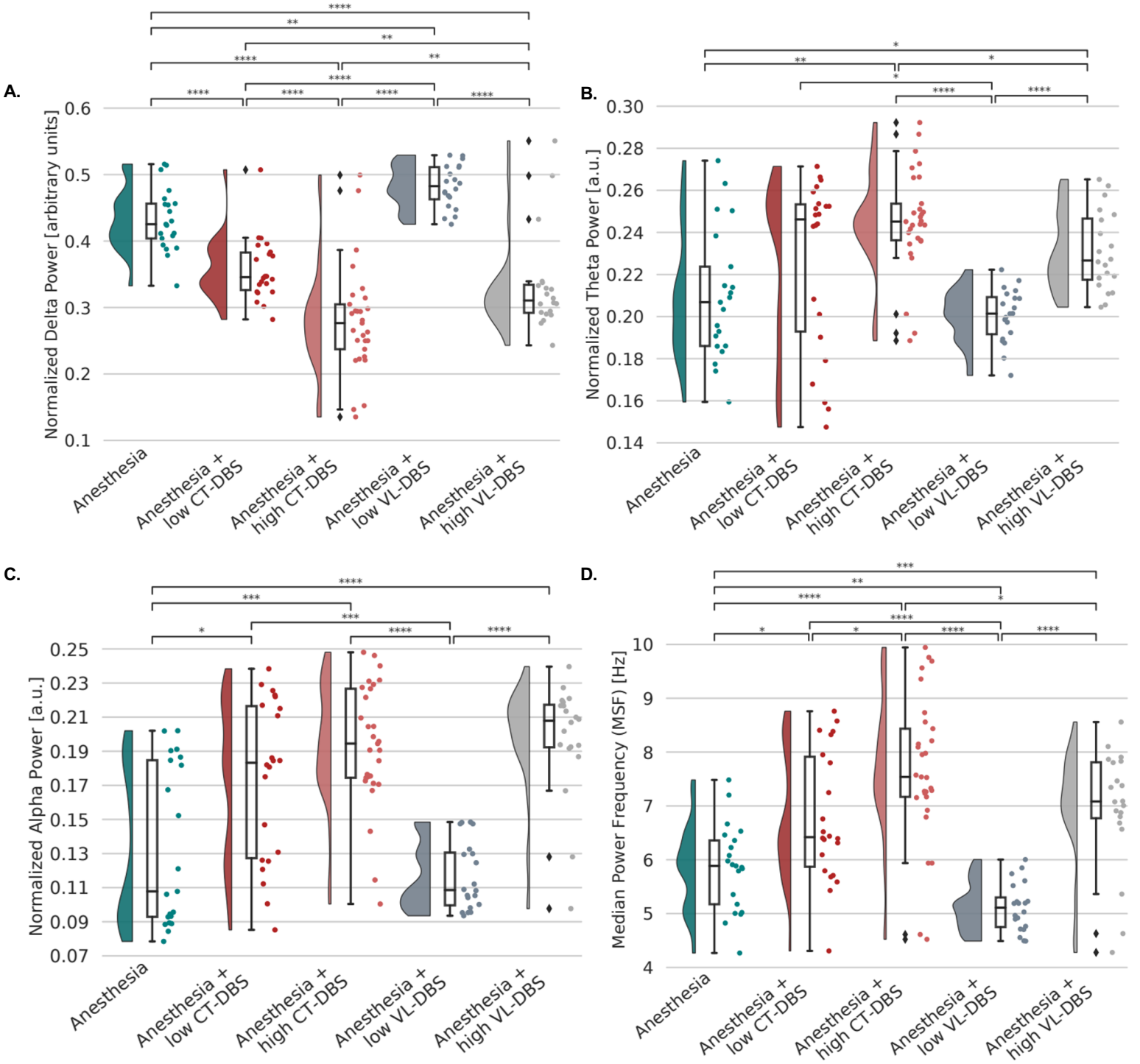

<u>Figure S5</u>: Modulation of normalized spectral power and median power frequency in the DBS conditions compared to anesthesia.

Distributions of the average values of normalized spectral power of (A) delta (1-4 Hz), (B) theta (4-8 Hz) and (C) alpha (8-13 Hz) oscillatory bands and (D) median power frequency (MSF) calculated on the epochs of the four stimulation conditions and under anesthesia. MSF is the frequency that divides the power spectrum in two equal areas. The figures consist of a distribution - smoothened version of a histogram, a box plot and a representation of the data points. Each dot in the figure represents the average value of a given marker across epochs during one recording session. a.u., arbitrary units. The significance lines represent FDR corrected Mann-Whitney U two-sided tests (see Methods). p-value annotation legend: ns: 5.00e-02 < p <= 1.00e+00, *: 1.00e-02 < p <= 5.00e-02, **: 1.00e-03 < p <= 1.00e-02, ***: 1.00e-04 < p <= 1.00e-03, ****: p <= 1.00e-04. P-values are FDR corrected.

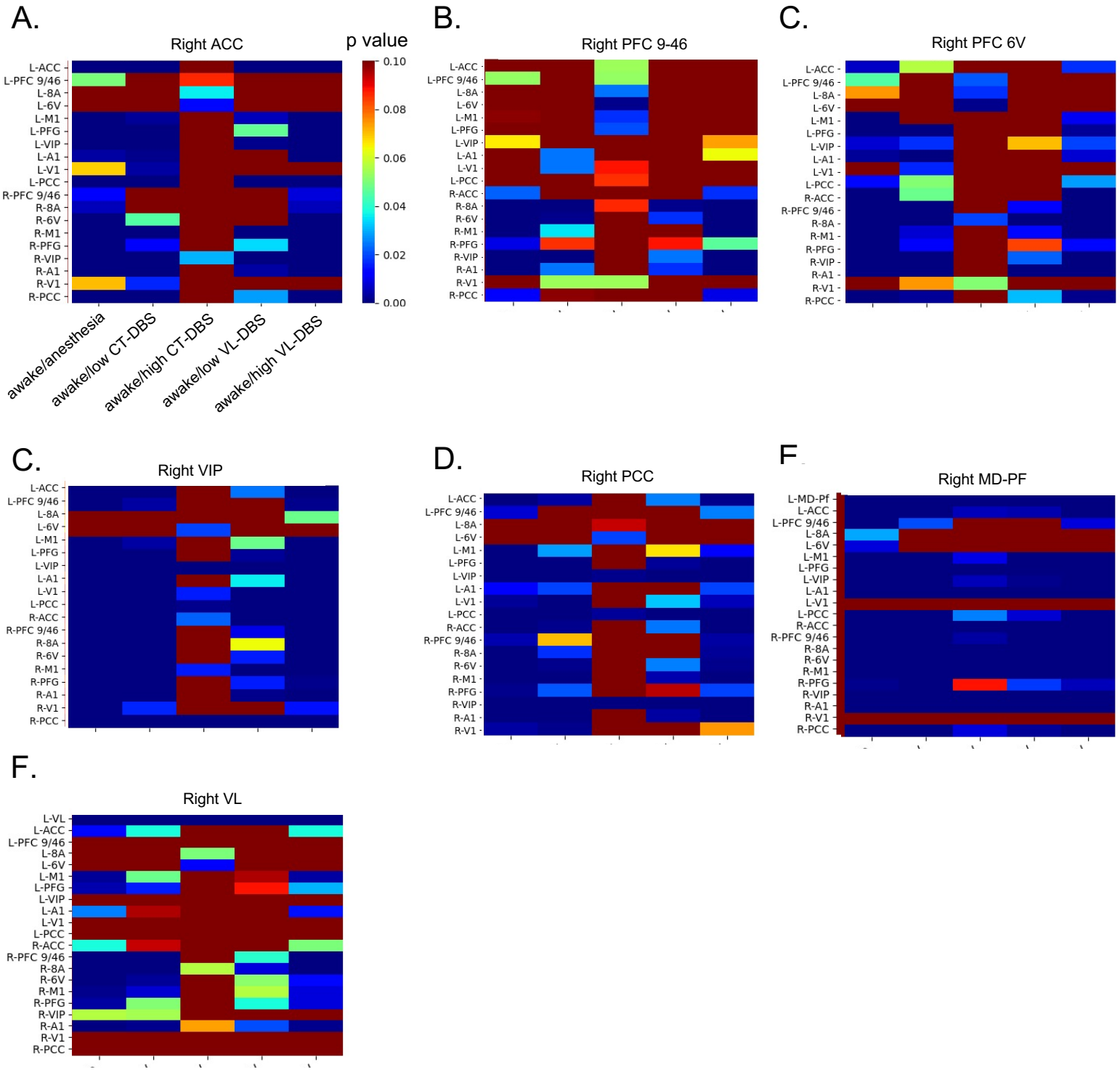

<u>Figure S6</u>: p values matrices for the ANOVA comparison of the awake state versus different experimental conditions of the static functional correlations within the macaque Global Neuronal Workspace (GNW) nodes and sensori-motor areas.

Statistical p values obtained by ANOVA to compare static functional correlations within the macaque GNW nodes and sensori-motor areas in the different experimental conditions. X-axis displays the experimental conditions (awake, anesthesia, low central thalamic (CT) DBS, high CT-DBS, low ventral-lateral thalamic (VL) DBS and high VL-DBS states), y-axis represents the macaque GNW areas correlated to the seed ($p < 0.001$, FDR corrected). For each region, the matrix stands for the p value for the comparison of the awake state versus anesthesia, low CT-DBS, high CT-DBS, low VL-DBS and high VL-DBS between the seed and the rest of the macaque GNW nodes and sensori-motor areas.

Anterior cingulate cortex (ACC) ; Prefrontal cortex (area 9/46, 8A, 6 Ventral) ; Primary motor cortex (M1) ; Parietal cortex (area PFG) ; Ventral Intraparietal sulcus (VIP) ; Primary auditory cortex (A1) ; Primary visual area (V1) ; Posterior cingulate cortex (PCC).

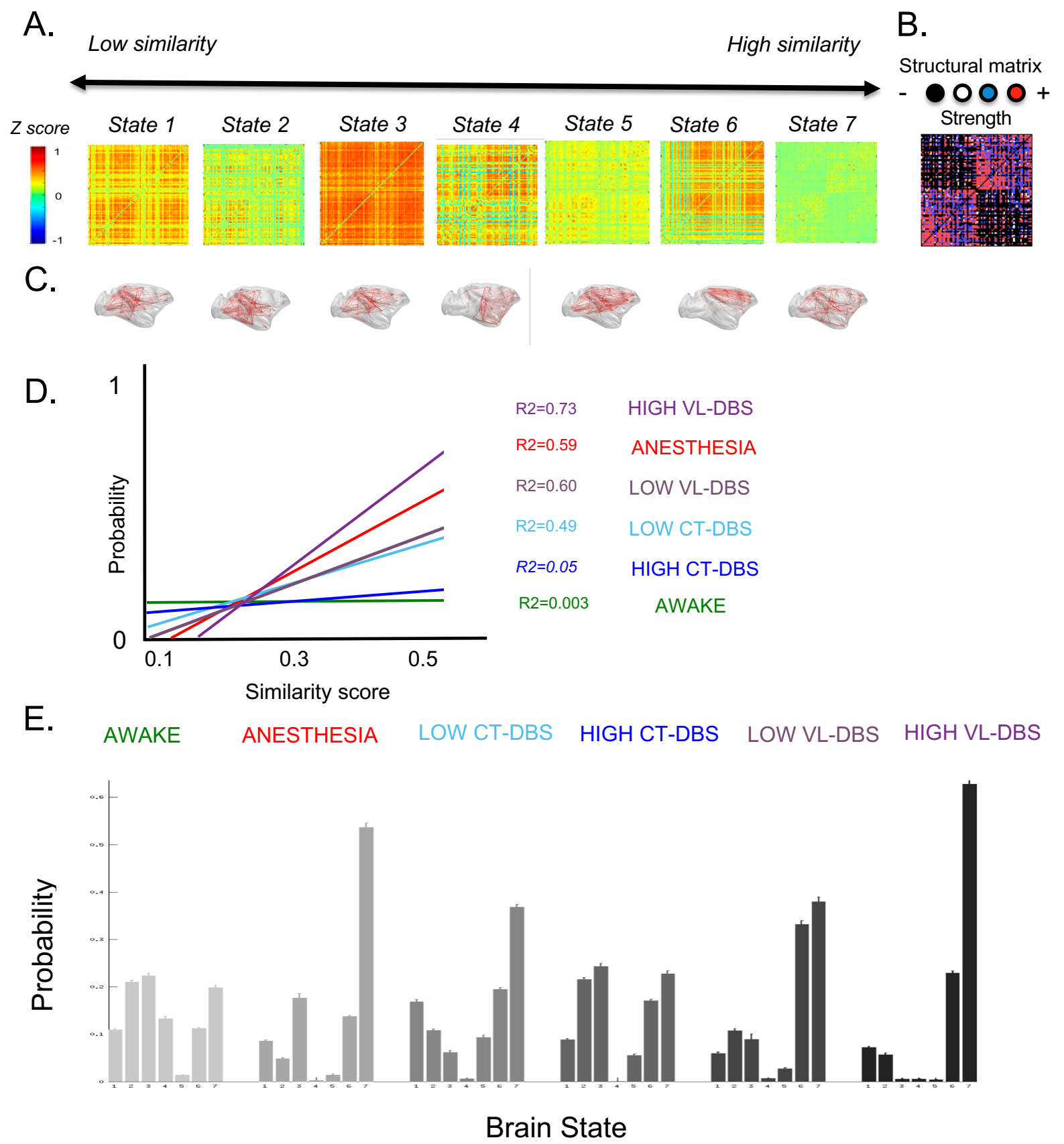

Figure S7: DBS effect on cortical dynamical correlations

(A) Seven functional brain states obtained by unsupervised clustering of the Z score matrix (all conditions pooled together, awake state, anesthesia, low central thalamic (CT) DBS, high CT-DBS, low ventral-lateral thalamic (VL) DBS and high VL-DBS). (B) Structural connectivity matrix derived from the CoCoMac atlas of anatomical macaque cortical connectivity. Colors represent the four grades of connection intensity (black=0; white=1; blue=2 and red=3). (C) Brain renders displaying the 400 strongest links for each functional brain state. Red line represent positive connections between regions of interests; blue represent negative connections. (D) Probability of occurrence of each functional brain state as a function of the similarity with the structural connectivity, for the awake state (green), anesthesia (red), low CT-DBS (light blue), high CT-DBS (dark blue), low VL-DBS (light purple) and high VL-DBS (dark purple). (E) Probability distributions of functional brain states for the for the awake state (green), anesthesia (red), low CT-DBS (light blue), high CT-DBS (dark blue), low VL-DBS (light purple) and high VL-DBS (dark purple). Error bars stand for 1 SEM.

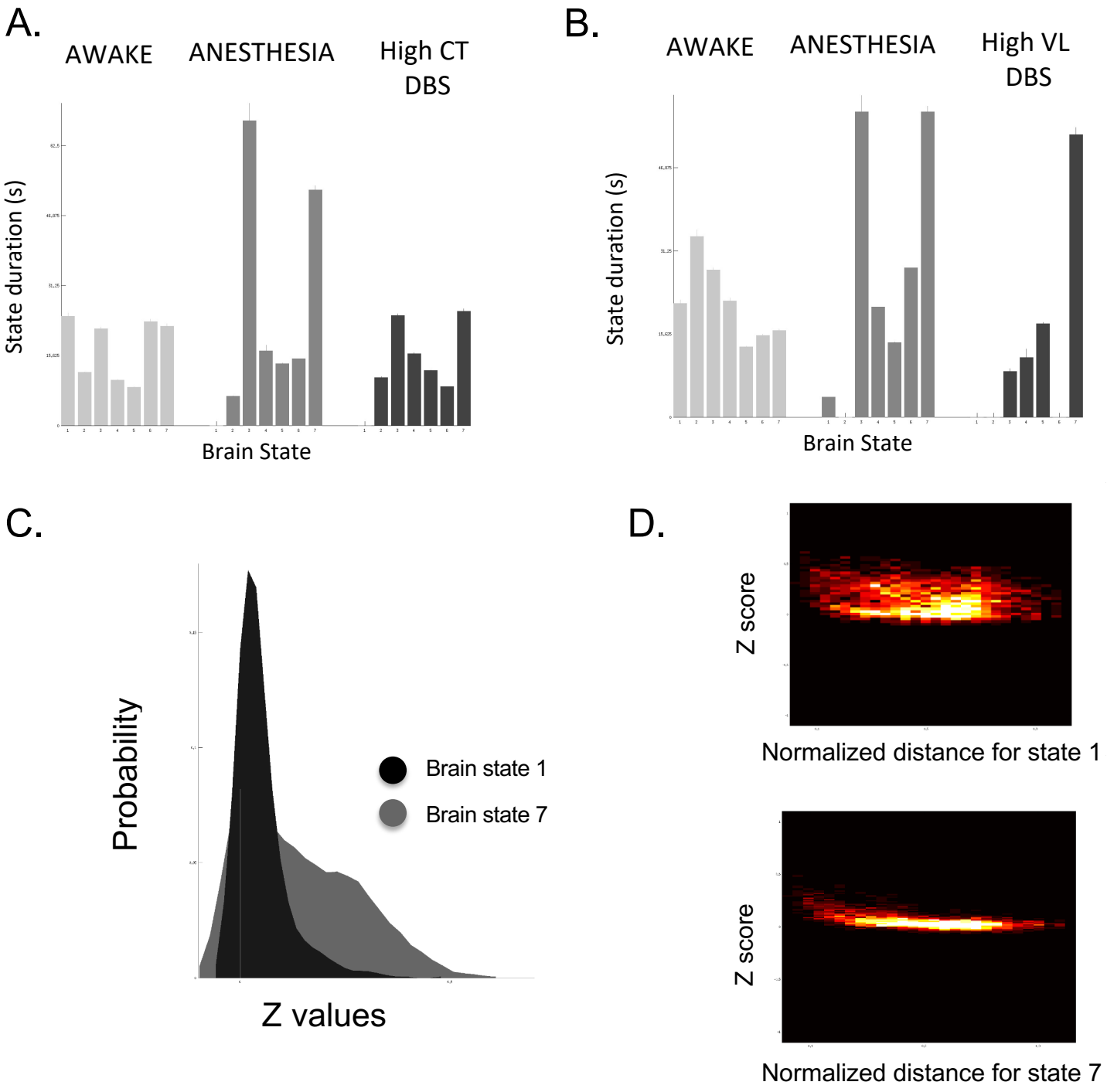

<u>Figure S8</u>: Average life time of brain states in the awake state, under anesthesia and during high cental thalamic (CT) DBS (left) or high ventral-lateral thalamic (VL) DBS (right); normalized probability distribution and two-dimensional normalized histograms

Average life time of brain states for the awake, anesthesia and high central thalamic (CT) DBS condition (A) or high ventral-lateral thalamic (VL) DBS (B) for 7 brain states obtained by k-means clustering. Error bars stand for 1 SEM. Normalized probability distribution of all Z values for the functional brain state 1 (the least similar to the structural brain connectivity) and functional brain state 7 (the most similar to the structural brain connectivity) for awake, anesthesia and high CT-DBS resting state pooled together. Similar results were obtained regardless the inputs conditions for the clustering (C). Two-dimensional normalized histograms for functional brain state 1 and functional brain state 7 for the clustering of awake, anesthesia and high CT-DBS condition. (D) Z values as a function of distance between pairs of regions of interest for brain state 1 (upper right) and brain state 7 (lower right) for the clustering of awake, anesthesia and high CT-DBS condition.

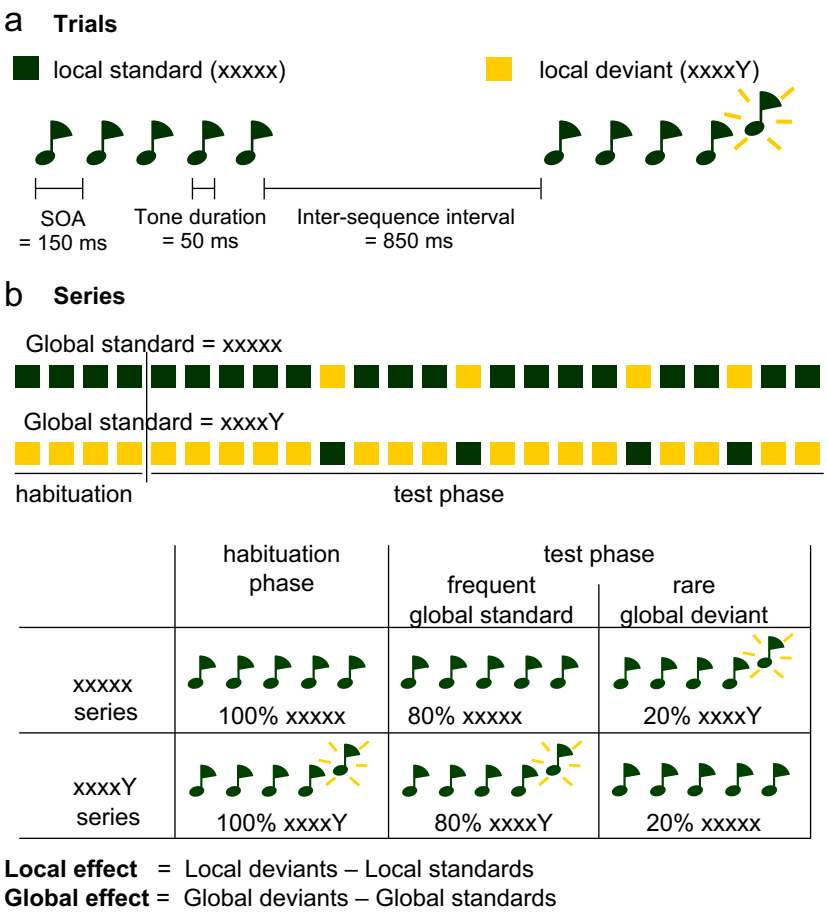

Figure S9: Local-global auditory paradigm

Description of the event-related auditory paradigm called local-global used in the auditory event-related fMRI experiments. Local deviants occur at the trial level (1st order) whereas Global deviants occur at the series level (2nd order).

fMRI activations during the auditory "Local-global" experiment

Local effect: High CT- DBS > Anesthesia

Individual results: Monkey N

A.

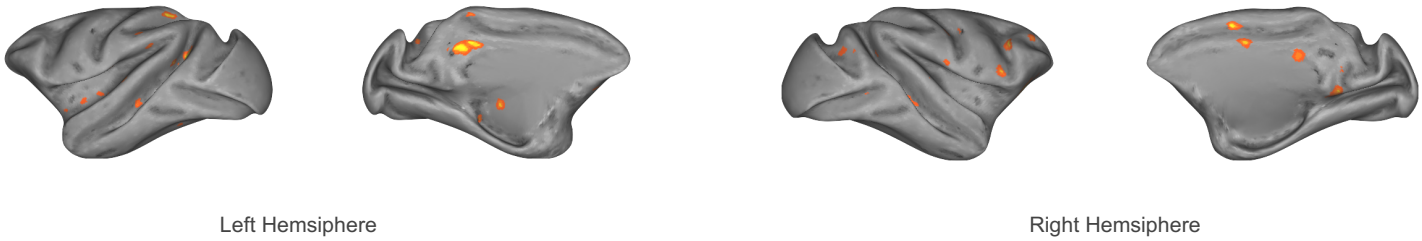

Left Hemisphere Right Hemisphere

B.

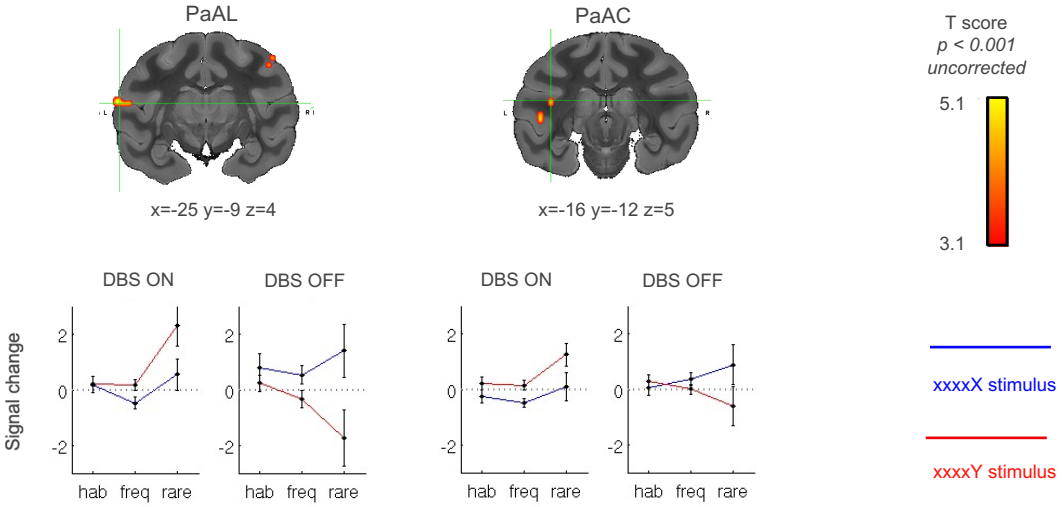

Individual results: Monkey T

C.

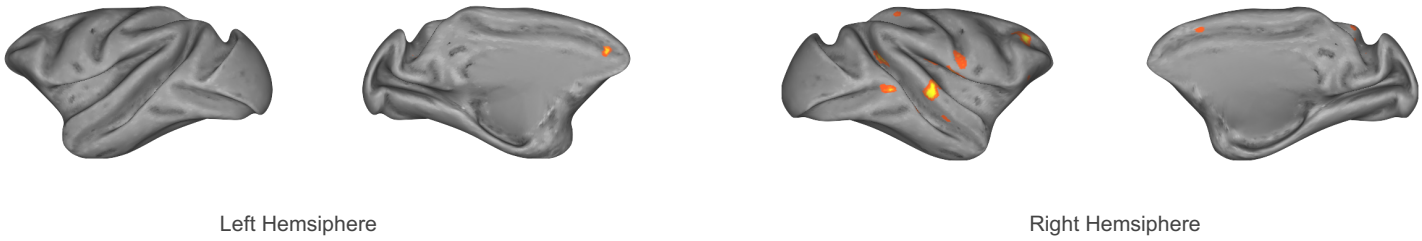

Left Hemisphere Right Hemisphere

D.

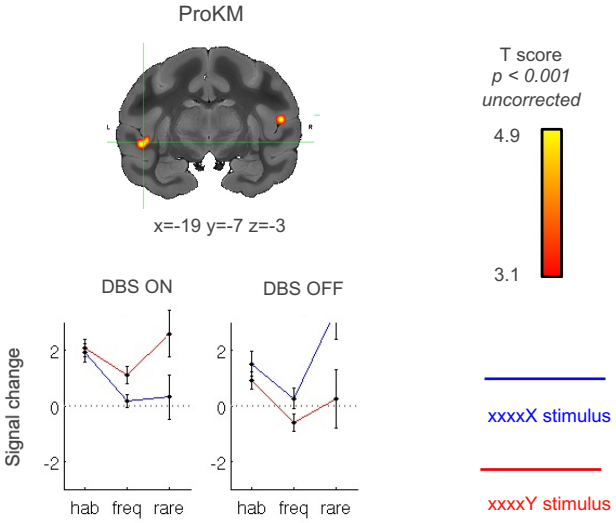

<u>Figure S10</u>: Activations maps for the local effect showing stronger activations under high central thalamic (CT) DBS compared to anesthesia state

Activation maps for the local effect showing stronger activations under high CT-DBS compared to anesthesia state (A, C). fMRI signal changes in areas responsive to the local effect (green cursor) (B,D). Individual results for monkey N (top panel - A,B) and monkey T (lower panel - C,D), p < 0.001, uncorrected.

PaAL, paraauditory cortex, lateral part; PaAc, paraauditroy cortex, caudal part; ProKM, auditory cortex, prokonio cortex , medial part.

fMRI activations during the auditory "Local-global" experiment

Global effect: High CT-DBS > Anesthesia

Individual results: Monkey N

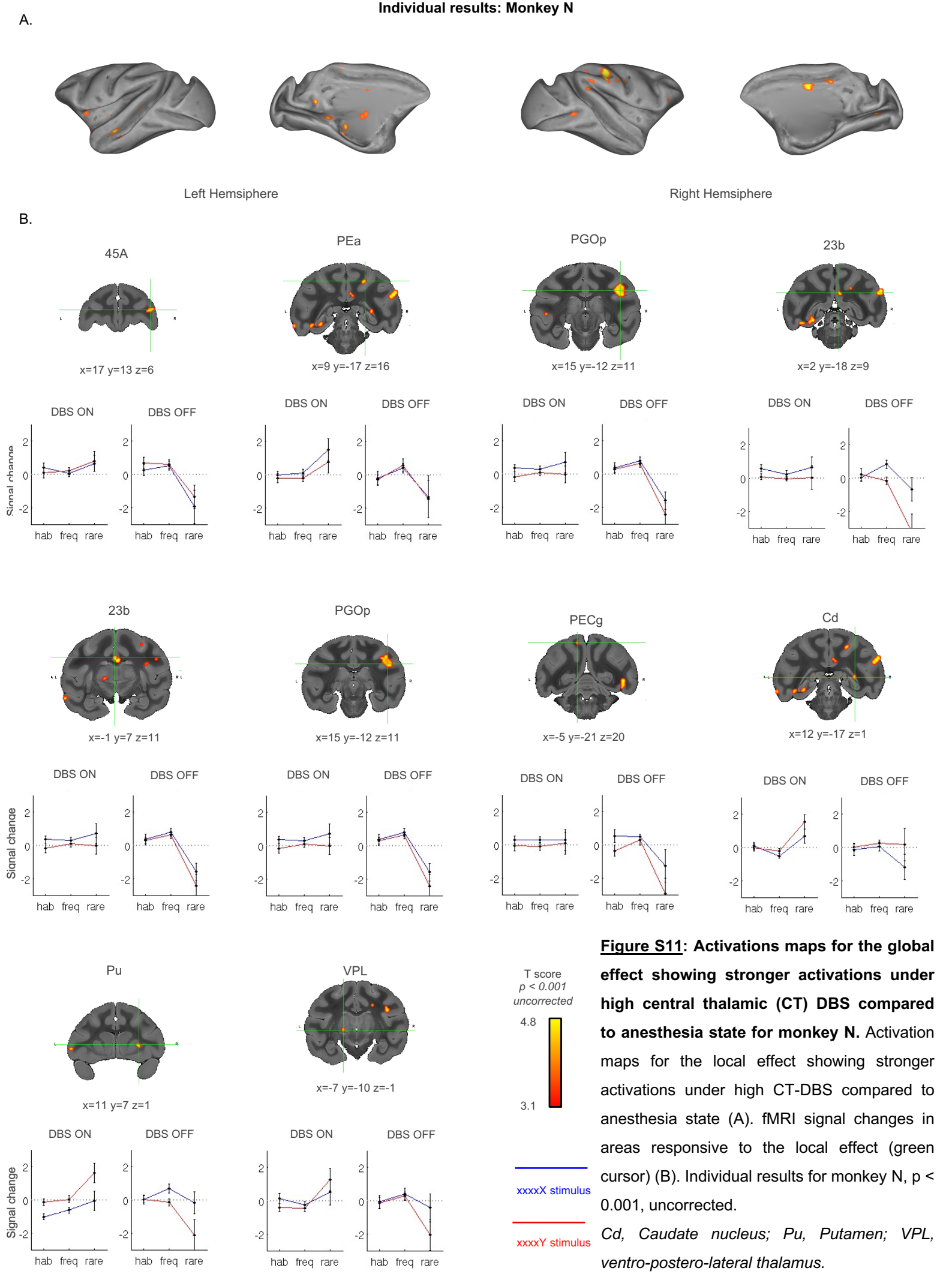

<u>Figure S11</u>: Activations maps for the global effect showing stronger activations under high central thalamic (CT) DBS compared to anesthesia state for monkey N. Activation maps for the local effect showing stronger activations under high CT-DBS compared to anesthesia state (A). fMRI signal changes in areas responsive to the local effect (green cursor) (B). Individual results for monkey N, p < 0.001, uncorrected.

Cd, Caudate nucleus; Pu, Putamen; VPL, ventro-postero-lateral thalamus.

fMRI activations during the auditory "Local-global" experiment

Global effect: High CT-DBS > Anesthesia

Individual results: Monkey T

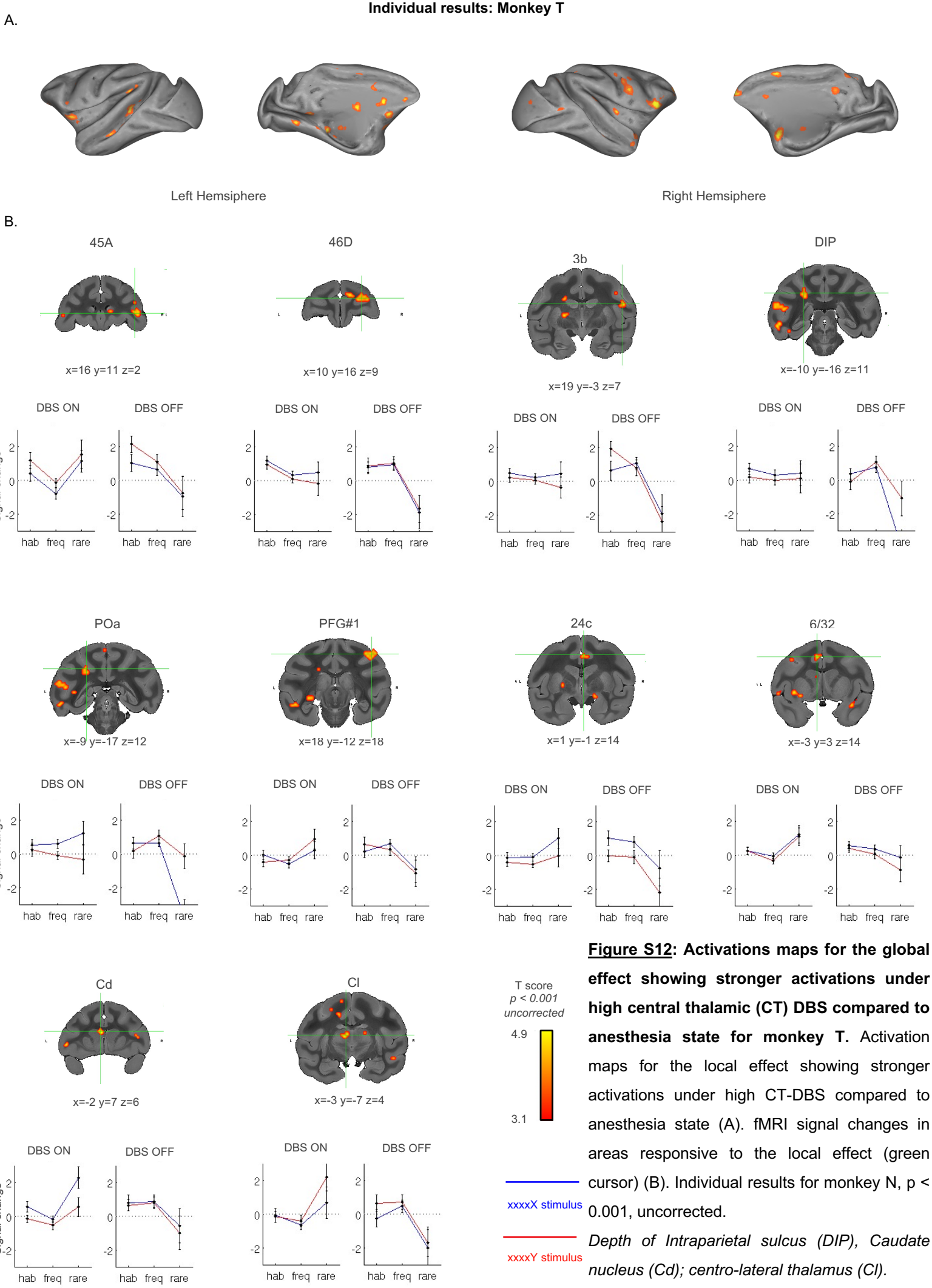

Figure S12: Activations maps for the global effect showing stronger activations under high central thalamic (CT) DBS compared to anesthesia state for monkey T. Activation maps for the local effect showing stronger activations under high CT-DBS compared to anesthesia state (A). fMRI signal changes in areas responsive to the local effect (green cursor) (B). Individual results for monkey N, p < 0.001, uncorrected.

Depth of Intraparietal sulcus (DIP), Caudate nucleus (Cd); centro-lateral thalamus (Cl).

Simulation of the thalamic nuclei activated during the DBS experiments

Thalamic nuclei	Abbreviation	CT-DBS				VL-DBS			
		low		high		low		high	
		monkey N	monkey T	monkey N	monkey T	monkey N	monkey T	monkey N	monkey T
Ventral-Postero-Medial	VPM	X	X	X	X		X	X	X
Centro-Median, Medial part	CMM	X	X	X	X				X
Centro-Median, Lateral part	CML	X	X	X	X				X
Medio-Dorsal, Central part	MDC	X	X	X	X		X	X	X
Ventral-Postero-Lateral	VPL			X	X	X	X	X	X
Medio-Dorsal, Lateral part	MDL			X	X	X	X	X	X
Ventral-Lateral, Medial part	VLM			X	X	X	X	X	X
Medio-Dorsal-Medial part	MDM			X	X				X
Inter-Medio-Dorsal	IMD			X	X				
Centro-Lateral	CL					X	X	X	X
Medio-Dorsal, Dorsal part	MDD					X		X	
Lateral-Dorsal, SuperFicial part	LDSF							X	
Ventral-Anterior, Lateral part	VAL							X	X
Ventral-Lateral, Lateral part	VLL							X	

Table S1: Simulation of the stimulated thalamic nuclei around the DBS lead using the LEAD DBS macaque toolbox

Estimation of the thalamic nuclei that were included in the volume of activated tissue around the DBS lead active contact*(71)* for monkey N and monkey T across the four experimental conditions (low central thalamic (CT) DBS, high CT-DBS, low ventral thalamic (VL) DBS and high VL-DBS).

Physiological data during the resting state fMRI experiments

Condition	Animal	Heart Rate	Oxygen Saturation	Blood pressure			Respiration Rate	End-tidal CO_2	Temperature
				Systolic	Diastolic	Mean			
		(HR in bpm)	*(SpO_2 in %)*	*(SBP in mmHg)*	*(DBP in mmHg)*	*(MBP in mmHg)*	*(RR in breath/min)*	*($EtCO_2$ in mmHg)*	*(T in °C)*
Anesthesia	monkey N	111	98	116	59	87	20	41	37.0
		± 9	*± 2*	*± 10*	*± 7*	*± 9*	*± 1*	*± 2*	*± 0.7*
	monkey T	116	97	95	46	68	18	37	38.3
		± 17	*± 3*	*± 8*	*± 7*	*± 9*	*± 2*	*± 2*	*± 0.7*
Low CT-DBS	monkey N	134	99	128	70	101	21	43	37.1
		± 13	*± 1*	*± 13*	*± 12*	*± 13*	*± 2*	*± 2*	*± 0.3*
	monkey T	123	99	98	47	71	18	39	38.6
		± 18	*± 1*	*+/- 12*	*+/- 6*	*+/- 8*	*+/- 2*	*+/- 2*	*+/- 0.5*
High CT-DBS	monkey N	164	98	129	71	99	21	45	37.3
		± 16	*± 2*	*± 15*	*± 15*	*± 14*	*± 1*	*± 3*	*± 0.4*
	monkey T	181	98	133	74	104	19	43	39.6
		+/- 19	*+/- 2*	*+/- 12*	*+/- 12*	*+/- 13*	*+/- 2*	*+/- 2*	*+/- 0.4*
Low VL-DBS	monkey T	145	98	113	54	81	19	38	39.0
		± 3	*± 2*	*± 14*	*± 12*	*± 12*	*± 2*	*± 1*	*± 0.5*
High VL-DBS	monkey T	163	98	127	71	99	18	42	39.1
		± 14	*± 1*	*± 15*	*± 19*	*± 19*	*± 2*	*± 2*	*± 0.6*

Table S2: Physiological data during the fMRI resting-state experiments.

Oxygen saturation (SpO_2); systolic, diastolic and mean blood pressure (respectively SBP, DBP, MBP); respiration rate (RR); end-tidal CO_2 ($EtCO_2$) and temperature (T) for each animal (monkey N and T) under general anesthesia, general anesthesia plus low central thalamic (CT) DBS, general anesthesia plus high CT-DBS, general anesthesia plus low ventral-lateral thalamic (VL) DBS and general anesthesia plus high VL-DBS.

fMRI activations during the DBS block-design experiment

			CT-DBS				VL-DBS			
			low		high		low		high	
Area	**Abbreviation**	**Hemisphere**	**T score**	**p value**	**T score**	**p value**	**T score**	**p value**	**T score**	**p value**
Orbitofrontal cortex										
Area 13 of cortex	13	Right		*n.s*	19.15	$p_{FWE} < 1x10\text{-}12$		*n.s*		*n.s*
Area 13a of cortex	13a	Left	5.11	$p_{FW} = 7.4x10\text{-}3$	5.11	$p_{FWE} = 7.4x10\text{-}3$		*n.s*		*n.s*
Area 14o	14o	Right		*n.s*	5.91	$p_{FWE} = 1.21x10\text{-}4$		*n.s*		*n.s*
Area 25 of cortex	25	Left	5.48	$p_{FWE} = 9.66x10\text{-}4$	5.48	$p_{FWE} = 9.66x10\text{-}4$		*n.s*		*n.s*
Orbitofrontal cortex	OPro	Right		*n.s*	19.15	$p_{FWE} < 1x10\text{-}12$		*n.s*		*n.s*
Frontal cortex										
Are 4 of cortex (primary motor)	4#1	Left		*n.s*	18.47	$p_{FWE} < 1x10\text{-}12$		*n.s*		*n.s*
		Right		*n.s*	18.47	$p_{FWE} < 1x10\text{-}12$		*n.s*	9.94	$p_{FWE} < 1x10\text{-}12$
Area 6 of cortex, Medial part (supplementary motor)	6M	Left		*n.s*	19.15	$p_{FWE} < 1x10\text{-}12$		*n.s*		*n.s*
		Right		*n.s*	19.15	$p_{FWE} < 1x10\text{-}12$		*n.s*	5.77	$p_{FWE} = 2.67x10\text{-}4$
Area 6 of cortex, DorsoCaudal part (Matellis F2)	6DC	Right		*n.s*	18.47	$p_{FWE} < 1x10\text{-}12$		*n.s*	12.81	$p_{FWE} < 1.0x10\text{-}12$
Area 6 of cortex, DorsoRostral part Matellis F7)	6DR	Right		*n.s*	19.15	$p_{FWE} < 1x10\text{-}12$		*n.s*	12.81	$p_{FWE} < 1.0x10\text{-}12$
Area 6 of cortex, Ventral part, Caudal subdivision (Matellis F4)	6VC	Left		*n.s*	6.54	$p_{FWE} = 2.37x10\text{-}6$		n.s		*n.s*
		Right		*n.s*	18.47	$p_{FWE} < 1x10\text{-}12$		*n.s*		*n.s*
Area 6 of cortex, Ventral part, Rostral subdivision (Matellis F5)	6VR	Left		*n.s*	6.16	$p_{FWE} = 2.54x10\text{-}5$		*n.s*		*n.s*
		Right		*n.s*	19.15	$p_{FWE} < 1x10\text{-}12$		*n.s*	5.61	$p_{FWE} = 6.87x10\text{-}4$
Area 6/32 of cortex	6 32	Left		*n.s*	19.15	$p_{FWE} < 1x10\text{-}12$		*n.s*		*n.s*
		Right	4.96	$p_{FWE} = 1.56x10\text{-}2$	19.15	$p_{FWE} < 1x10\text{-}12$		*n.s*	5.77	$p_{FWE} = 2.67x10\text{-}4$
Area 8A of cortex	8A	Left		*n.s*	5.79	$p_{FWE} = 2.41x10\text{-}4$		*n.s*		*n.s*
		Right		*n.s*	18.47	$p_{FWE} < 1x10\text{-}12$		*n.s*	12.81	$p_{FWE} < 1.0x10\text{-}12$
Area 8of cortex, AnteroDorsal part	8AD	Left		*n.s*	7.10	$p_{FWE} = 5.04x10\text{-}8$		n.s		*n.s*
		Right	5.92	$p_{FWE} = 7.47x10\text{-}5$	18.47	$p_{FWE} < 1x10\text{-}12$		*n.s*	12.81	$p_{FWE} < 1.0x10\text{-}12$
Area 8 of cortex, AnteroVentral part	8AV	Right		*n.s*	19.15	$p_{FWE} < 1x10\text{-}12$		*n.s*	12.81	$p_{FWE} < 1.0x10\text{-}12$
Area 8B of cortex	8B	Left		*n.s*	7.10	$p_{FWE} = 5.04x10\text{-}8$		*n.s*		*n.s*
		Right		*n.s*	18.47	$p_{FWE} < 1x10\text{-}12$		*n.s*		*n.s*
Area 8/32 of cortex	8 32	Right		*n.s*	19.15	$p_{FWE} < 1x10\text{-}12$		*n.s*		*n.s*
Area 9 of cortex, Medial part	9M	Left		*n.s*	18.47	$p_{FWE} < 1x10\text{-}12$		*n.s*		*n.s*
		Right		*n.s*	14.54	$p_{FWE} < 1x10\text{-}12$		*n.s*		*n.s*
Area 9/32 of cortex	9 32	Right	7.72	$p_{FDR} = 2.84x10\text{-}10$		$p_{FDR} = 2.84x10\text{-}10$		*n.s*		*n.s*
Area 9/46 of cortex	9 46	Right	6.98	$p_{FWE} = 7.08x10\text{-}8$	19.15	$p_{FWE} < 1x10\text{-}12$		*n.s*	9.94	$p_{FWE} < 1x10\text{-}12$
Area 44 of cortex	44	Left		*n.s*	6.66	$p_{FWE} = 1.03x10\text{-}6$		*n.s*		*n.s*
		Right		*n.s*	19.15	$p_{FWE} < 1x10\text{-}12$		*n.s*	9.94	$p_{FWE} < 1x10\text{-}12$
Area 45A of crotex	45A	Right	7.30	$p_{FWE} = 7.23x10\text{-}9$	19.15	$p_{FWE} < 1x10\text{-}12$		*n.s*	9.94	$p_{FWE} < 1.0x10\text{-}12$
Area 45B of cortex	45B	Left		*n.s*	6.66	$p_{FWE} = 1.03x10\text{-}6$		*n.s*		*n.s*
		Right	7.30	$p_{FWE} = 7.23x10\text{-}9$	19.15	$p_{FWE} < 1x10\text{-}12$		*n.s*	9.94	$p_{FWE} < 1.0x10\text{-}12$
Area 46D of cortex	46D	Right	6.98	$p_{FWE} = 7.08x10\text{-}8$		$p_{FWE} = 7.08x10\text{-}8$		*n.s*		*n.s*
Area 46V of cortex	46V	Left		*n.s*	5.27	$p_{FWE} = 4.68x10\text{-}3$		*n.s*		*n.s*
		Right	6.98	$p_{FWE} = 7.08x10\text{-}8$		$p_{FWE} = 7.08x10\text{-}8$		*n.s*		*n.s*
Area 47 (old 12) of cortex, Lateral part	47L	Left	6.27	$p_{FWE} = 8.28x10\text{-}6$		$p_{FWE} = 8.28x10\text{-}6$		*n.s*		*n.s*
Area 47 (old 12) of cortex, Orbital part	47O	Left		*n.s*	6.66	$p_{FWE} = 1.03x10\text{-}6$		*n.s*		*n.s*
Area ProM (promotor)	ProM#1	Left		*n.s*	11.36	$p_{FWE} < 1x10\text{-}12$		*n.s*		*n.s*

fMRI activations during the DBS block-design experiment

Area	Abbreviation	Hemisphere	CT-DBS low T score	CT-DBS low p value	CT-DBS high T score	CT-DBS high p value	VL-DBS low T score	VL-DBS low p value	VL-DBS high T score	VL-DBS high p value
Parietal cortex										
Area 1 of cortex (somatosensory)	1	Left		*n.s*	18.47	$p_{FWE} < 1x10-12$		*n.s*		*n.s*
		Right		*n.s*	18.47	$p_{FWE} < 1x10-12$		*n.s*	9.94	$p_{FWE} < 1x10-12$
Area 2 of cortex (somatosensory)	2#1	Left		*n.s*	18.47	$p_{FWE} < 1x10-12$		*n.s*		*n.s*
		Right		*n.s*	18.47	$p_{FWE} < 1x10-12$		*n.s*	12.81	$p_{FWE} < 1x10-12$
Area 2 of cortex, Vesticular part	2Ve			*n.s*	18.47	$p_{FWE} < 1x10-12$		*n.s*		*n.s*
Area 3a of cortex (somatosensory)	3a	Left		*n.s*	18.47	$p_{FWE} < 1x10-12$		*n.s*		*n.s*
		Right		*n.s*	18.47	$p_{FWE} < 1x10-12$		*n.s*	9.94	$p_{FWE} < 1x10-12$
Area 3b of cortex (somatosensory)	3b	Right		*n.s*	18.47	$p_{FWE} < 1x10-12$		*n.s*	16.05	$p_{FWE} < 1.0x10-12$
Depth IntraParietal area	DIP	Right		*n.s*	18.47	$p_{FWE} < 1x10-12$		*n.s*		*n.s*
Dorsal parietal area	Dpt	Left		*n.s*	7.27	$p_{FWE} = 1.53x10-8$		*n.s*	7.23	$p_{FWE} = 2.09x10-8$
		Right	5.73	$p_{FWE} = 2.32x10-4$	18.47	$p_{FWE} < 1x10-12$		*n.s*		*n.s*
OccipitoParietal area	OPt	Left		*n.s*	12.59	$p_{FWE} < 1x10-12$		*n.s*		*n.s*
		Right		*n.s*	18.47	$p_{FWE} < 1x10-12$		*n.s*		*n.s*
Parietal area PE	PE	Right	6.51	$p_{FWE} = 1.72x10-6$	18.47	$p_{FWE} < 1x10-12$		*n.s*	7.26	$p_{FWE} = 1.72x10-8$
Parieral area PE, Caudal part	PEC	Right		*n.s*	5.39	$p_{FWE} = 2.3x10-3$		*n.s*	7.85	$p_{FWE} = 2.08x10-10$
Parietal area PEa	PEa	Right	6.30	$p_{FWE} = 7.07x10-6$	18.47	$p_{FWE} < 1x10-12$		*n.s*	7.85	$p_{FWE} = 2.08x10-10$
Parietal area PF (cortex)	PFCx	Right		*n.s*		*n.s*		*n.s*	9.94	$p_{FWE} < 1x10-12$
Parieal area PF, Opercular part	PFOp	Left		*n.s*	7.27	$p_{FWE} = 1.53x10-8$		*n.s*		*n.s*
		Right		*n.s*	18.47	$p_{FWE} < 1x10-12$		*n.s*		*n.s*
Parietal area PG	PG	Right		*n.s*	12.62	$p_{FWE} < 1x10-12$		*n.s*		*n.s*
Parieal area PG, Opercular part	PGOp	Left		*n.s*	7.27	$p_{FWE} = 1.53x10-8$		*n.s*		*n.s*
		Right	7.38	$p_{FWE} = 3.90x10-9$	18.47	$p_{FWE} < 1x10-12$		*n.s*	5.95	$p_{FWE} = 9.51x10-5$
Parietal area POa, External part	POaE	Right		*n.s*	18.47	$p_{FWE} < 1x10-12$		*n.s*		*n.s*
Parietal area POa, Internal part	POaI	Right		*n.s*	18.47	$p_{FWE} < 1x10-12$		*n.s*		*n.s*
ParietoOccipital associated area in the intraparietal sulcus	POa	Left		*n.s*	7.27	$p_{FWE} = 1.53x10-8$		*n.s*		*n.s*
		Right		*n.s*	18.47	$p_{FWE} < 1x10-12$		*n.s*	9.94	$p_{FWE} < 1x10-12$
Posterior Parietal area	PPt	Right		*n.s*	18.47	$p_{FWE} < 1x10-12$		*n.s*		*n.s*
RetroInsular area, Parietal part	ReIP	Left		*n.s*	7.27	$p_{FWE} = 1.53x10-8$		*n.s*		*n.s*
		Right		*n.s*	12.62	$p_{FWE} < 1x10-12$		*n.s*		*n.s*
Secondary somatosensory cortex	S2	Left		*n.s*	7.27	$p_{FWE} = 1.53x10-8$		*n.s*		*n.s*
		Right		*n.s*	18.47	$p_{FWE} < 1x10-12$		*n.s*	5.66	$p_{FWE} = 5.12x10-4$
Secondary somatosensory cortex, External part	S2E	Right		*n.s*		*n.s*		*n.s*	12.81	$p_{FWE} < 1x10-12$
Secondary somatosensory cortex, Internal part	S2I	Right		*n.s*	18.47	$p_{FWE} < 1x10-12$		*n.s*		*n.s*
Visual area 4, Dorsal part	V4D	Right		*n.s*	18.47	$p_{FWE} < 1x10-12$		*n.s*		*n.s*
Visual area 4, Transitional part	V4T	Right		*n.s*	18.47	$p_{FWE} < 1x10-12$		*n.s*		*n.s*
Visual area 4A	V4A	Left		*n.s*	7.27	$p_{FWE} = 1.53x10-8$		*n.s*	7.23	$p_{FWE} = 2.09x10-8$
		Right		*n.s*	18.47	$p_{FWE} < 1x10-12$		n.s		*n.s*
Cingulate cortex										
Area 23 of cortex	23	midline	6.84	$p_{FWE} = 1.82x10-7$		*n.s*		*n.s*		*n.s*
Area 23a of cortex	23a	midline		*n.s*	5.60	$p_{FWE} = 7.36x-4$		*n.s*		*n.s*
Area 23b of cortex	23b			*n.s*	18.47	$p_{FWE} < 1x10-12$		*n.s*		*n.s*
Area 23c of cortex	23c	Left		*n.s*	18.47	$p_{FWE} < 1x10-12$		*n.s*		*n.s*
		Right		*n.s*	18.47	$p_{FWE} < 1x10-12$		*n.s*		*n.s*
Area 24/23b of cortex	24 23b	Right		*n.s*	18.47	$p_{FWE} < 1x10-12$		*n.s*		*n.s*
Area 24/23c of cortex	24 23c	Left		*n.s*	18.47	$p_{FWE} < 1x10-12$		*n.s*		*n.s*
		Right		*n.s*		*n.s*		*n.s*	5.77	$p_{FWE} = 2.67x10-4$
Area 24b of cortex	24b	Left		*n.s*	18.47	$p_{FWE} < 1x10-12$		*n.s*		*n.s*
		Right		*n.s*	18.47	$p_{FWE} < 1x10-12$		*n.s*		*n.s*
Area 24c of cortex	24c	Left		*n.s*	18.47	$p_{FWE} < 1x10-12$		*n.s*		*n.s*
		Right	6.98	$p_{FWE} = 7.08x10-8$	18.47	$p_{FWE} < 1x10-12$		*n.s*		*n.s*
Area 24d of cortex	24d	Left		*n.s*	18.47	$p_{FWE} < 1x10-12$		*n.s*		*n.s*
Area 31 of cortex	31	Left		*n.s*	18.47	$p_{FWE} < 1x10-12$		*n.s*		*n.s*
		Right		*n.s*	18.47	$p_{FWE} < 1x10-12$		*n.s*		*n.s*
Area PGM/31 of cortex	PGM 31	midline	5.41	$p_{FWE} = 1.4x10-3$		*n.s*		*n.s*		*n.s*
Parietal area PE, Cingulate part	PECg	Right		*n.s*	18.47	$p_{FWE} < 1x10-12$		*n.s*		*n.s*

fMRI activations during the DBS block-design experiment

			CT-DBS				VL-DBS			
			low		high		low		high	
Area	**Abbreviation**	**Hemisphere**	**T score**	**p value**	**T score**	**p value**	**T score**	**p value**	**T score**	**p value**
Temporal cortex										
Area PG associated, region of superior temporal sulcus	PGa	Right		*n.s*	18.47	$p_{FWE} < 1x10-12$		*n.s*		*n.s*
Auditory Koniocortex, Lateral part	AKL	Left		*n.s*	7.27	$p_{FWE} = 1.53x10-8$		*n.s*		*n.s*
		Right		*n.s*	18.47	$p_{FWE} < 1x10-12$		*n.s*		*n.s*
Auditory Koniocortex, Medial part	AKM	Left		*n.s*	7.27	$p_{FWE} = 1.53x10-8$		*n.s*		*n.s*
		Right		*n.s*	18.47	$p_{FWE} < 1x10-12$		*n.s*		*n.s*
Fundus of Superior Temporal sulcus	FST	Left		*n.s*	6.48	$p_{FWE} = 3.37x10-6$		*n.s*		*n.s*
		Right		*n.s*	18.47	$p_{FWE} < 1x10-12$		*n.s*		*n.s*
Medial Superior Temporal area	MST	Left		*n.s*	7.27	$p_{FWE} = 1.53x10-8$		*n.s*		*n.s*
		Right		*n.s*	18.47	$p_{FWE} < 1x10-12$		*n.s*		*n.s*
Middle Temporal area (visual area 5)	MT	Left		*n.s*	7.27	$p_{FWE} = 1.53x10-8$		*n.s*		*n.s*
		Right		*n.s*	18.47	$p_{FWE} < 1x10-12$		*n.s*	6.08	$p_{FWE} = 4.26x10-5$
ParaAuditory area, Caudal part	PaAC	Left		*n.s*	7.27	$p_{FWE} = 1.53x10-8$		*n.s*		*n.s*
		Right		*n.s*	20.85	$p_{FWE} < 1x10-12$		*n.s*		*n.s*
ParaAuditory area, lateral part	PaAL	Right		*n.s*	18.47	$p_{FWE} < 1x10-12$		*n.s*		*n.s*
ParaAuditory area, Rostral part	PaAR	Right		*n.s*	12.62	$p_{FWE} < 1x10-12$		*n.s*		*n.s*
ProKoniocortex	ProK	Right		*n.s*	18.47	$p_{FWE} < 1x10-12$		*n.s*		*n.s*
RetroInsular area	ReI	Right		*n.s*	18.47	$p_{FWE} < 1x10-12$		*n.s*		*n.s*
RetroInsular area, Temporal part	ReIT	Left		*n.s*	7.27	$p_{FWE} = 1.53x10-8$		*n.s*		*n.s*
		Right		*n.s*	18.47	$p_{FWE} < 1x10-12$		*n.s*		*n.s*
Superior Temporal sulcus area 1	ST1	Right		*n.s*	8.83	$p_{FWE} < 1x10-12$		*n.s*		*n.s*
Superior Temporal area, gyral part	ST2g	Left		*n.s*	11.36	$p_{FWE} < 1x10-12$		*n.s*		*n.s*
Superior Temporal area, sulcal part	ST2s	Left		*n.s*	11.36	$p_{FWE} < 1x10-12$		*n.s*		*n.s*
Temporal area TAa	TAa	Right		*n.s*	18.47	$p_{FWE} < 1x10-12$		*n.s*		*n.s*
Temporal area TE, Medial part	TEM	Right		*n.s*	18.47	$p_{FWE} < 1x10-12$		*n.s*		*n.s*
Temporal area TE, OccipitoMedial part	TEOM	Right		*n.s*	18.47	$p_{FWE} < 1x10-12$		*n.s*		*n.s*
Temporal area TEa	TEa	Right		*n.s*	18.47	$p_{FWE} < 1x10-12$		*n.s*		*n.s*
Temporal ParietoOccipital associated area in sts	TPO	Right	7.38	$p_{FWE} = 3.90x10-9$	18.47	$p_{FWE} < 1x10-12$		*n.s*		*n.s*
Temporal ParietoOccipital associated area in sts, Caudal part	TPOC	Left		*n.s*	7.27	$p_{FWE} = 1.53x10-8$		*n.s*		*n.s*
		Right		*n.s*	18.47	$p_{FWE} < 1x10-12$		*n.s*		*n.s*
Temporoparietal cortex	Tpt	Left	5.02	$p_{FWE} = 1.15x10-2$		*n.s*		*n.s*		*n.s*
		Right	7.38	$p_{FWE} = 3.90x10-9$	18.47	$p_{FWE} < 1x10-12$		*n.s*		*n.s*
Occipital cortex										
Visual area 1 (primary visual cortex	V1	Left		*n.s*		*n.s*		*n.s*	9.22	$p_{FWE} < 1x10-12$
		Right	7.22	$p_{FWE} = 1.26x10-8$	18.47	$p_{FWE} < 1x10-12$		*n.s*	7.44	$p_{FWE} = 4.52x10-9$
Visual area 2	V2	Left		*n.s*	5.70	$p_{FWE} = 4.08x10-4$		*n.s*		*n.s*
		Right	8.65	$p_{FWE} < 1x10-12$	18.47	$p_{FWE} < 1x10-12$	7.97	$p_{FWE} = 3.94x10-11$	9.27	$p_{FWE} < 1x10-12$
Visual area 3, Dorsal part	V3D	Right		*n.s*	18.47	$p_{FWE} < 1x10-12$		*n.s*		*n.s*
Visual area 3A	V3A	Left		*n.s*	7.27	$p_{FWE} = 1.53x10-8$		*n.s*		*n.s*
		Right		*n.s*		*n.s*		*n.s*	5.63	$p_{FWE} = 6.10x10-4$
Insular cortex										
Dysgranular Insular cortex	DI	Left		*n.s*	6.18	$p_{FWE} = 2.29x10-5$		*n.s*		*n.s*
		Right		*n.s*	12.62	$p_{FWE} < 1x10-12$		*n.s*		*n.s*
Granular Insular cortex	GI	Left		*n.s*	7.52	$p_{FWE} = 2.54x10-9$		*n.s*		*n.s*
		Right		*n.s*	18.47	$p_{FWE} < 1x10-12$		*n.s*	5.32	$p_{FWE} = 1.54x10-2$
Insular Proisocortex	IPro	Right		*n.s*	12.32	$p_{FWE} < 1x10-12$		*n.s*		*n.s*
Striatum										
Caudate nucleus	Cd	Left		*n.s*	18.47	$p_{FWE} < 1x10-12$		*n.s*		*n.s*
		Right	6.34	$p_{FWE} = 5.50x10-6$	18.47	$p_{FWE} < 1x10-12$		*n.s*		*n.s*
Putamen	Pu	Left	5.30	$p_{FWE} = 2.6x10-3$	18.47	$p_{FWE} < 1x10-12$		*n.s*		*n.s*
		Right	13.68	$p_{FWE} < 1x10-12$	18.47	$p_{FWE} < 1x10-12$		*n.s*	5.30	$p_{FWE} = 3.7x10-3$

fMRI activations during the DBS block-design experiment

			CT-DBS				VL-DBS			
			low		high		low		high	
Area	**Abbreviation**	**Hemisphere**	**T score**	**p value**	**T score**	**p value**	**T score**	**p value**	**T score**	**p value**
Thalamus										
Lateral Geniculate Nucleus	LGN	Right		*n.s*	18.47	$p_{FWE} < 1x10\text{-}12$		*n.s*		*n.s*
Lateral pulvinar	Lpul	Left		*n.s*	5.20	$p_{FWE} = 1.44x10\text{-}2$		*n.s*		*n.s*
Medial Geniculate nucleus, Ventral part	MGV	Right		*n.s*	5.87	$p_{FWE} = 1.55x10\text{-}4$		*n.s*		*n.s*
Medial pulvinar	Mpul	Right	5.59	$p_{FWE} = 5.17x10\text{-}4$	11.07	$p_{FWE} < 1x10\text{-}12$		*n.s*		*n.s*
MedioDorsal thalamic nucleus, Central part	MDC	Left	5.65	$p_{FWE} = 3.56x10\text{-}4$	11.07	$p_{FWE} < 1x10\text{-}12$		*n.s*		*n.s*
MedioDorsal thalamic nucleus, Dorsal part	MDD	Left		*n.s*	11.07	$p_{FWE} < 1x10\text{-}12$		*n.s*		*n.s*
MediDorsal thalamic nucleus, Medial part	MDM	Left		*n.s*	11.07	$p_{FWE} < 1x10\text{-}12$		*n.s*		*n.s*
	PV	Left		*n.s*	11.07	$p_{FWE} < 1x10\text{-}12$		*n.s*		*n.s*
Paraventricular thalamic nucleus		Right		*n.s*	11.07	$p_{FWE} < 1x10\text{-}12$		*n.s*		*n.s*
	PVT	Left		*n.s*	11.07	$p_{FWE} < 1x10\text{-}12$		*n.s*		*n.s*
Paraventricular Thalamus		Right		*n.s*	11.07	$p_{FWE} < 1x10\text{-}12$		*n.s*		*n.s*
Reticular thalamic nucleus	R#4	Right		*n.s*	5.91	$p_{FWE} = 1.22x10\text{-}4$		*n.s*		*n.s*
Hypothalamus										
Hypothalamus	Hy	Left		*n.s*	14.54	$p_{FWE} < 1x10\text{-}12$		*n.s*		*n.s*
Pallidum										
External Globus Pallidus	EGP	Left		*n.s*	5.25	$p_{FWE} = 4.9x10\text{-}3$		*n.s*		*n.s*
Paraseptal subpallium										
Accumbens nucleus, Core	AcbC	Left		*n.s*	18.47	$p_{FWE} < 1x10\text{-}12$		*n.s*		*n.s*
		Right		*n.s*	18.47	$p_{FWE} < 1x10\text{-}12$		*n.s*		*n.s*
Accumbens nucleus, Shell	AcbSh	Left		*n.s*	18.47	$p_{FWE} < 1x10\text{-}12$		*n.s*		*n.s*
		Right		*n.s*	18.47	$p_{FWE} < 1x10\text{-}12$		*n.s*		*n.s*
Basal nucleus, Meynert	BM	Left		*n.s*	14.54	$p_{FWE} < 1x10\text{-}12$		*n.s*		*n.s*
Substancia Innominata	SI	Left		*n.s*	15.09	*pWE < 1x10-12*		*n.s*		*n.s*
Subpallial amygdala										
Anterior Amygdaloid area	AA	Left		*n.s*	14.54	$p_{FWE} < 1x10\text{-}12$		*n.s*		*n.s*
Bed nucleus of the Stria Terminallis IntraAmygdaloid	BSTIA	Left		*n.s*	15.09	$p_{FWE} < 1x10\text{-}12$		*n.s*		*n.s*
Central amygdaloid nucleus, Lateral division	CeL	Left		*n.s*	14.54	$p_{FWE} < 1x10\text{-}12$		*n.s*		*n.s*
Central amygdaloid nucleus, Medial division	CeM	Left		*n.s*	14.54	$p_{FWE} < 1x10\text{-}12$		*n.s*		*n.s*
Ventral pallium										
BasoMedial amygdaloid nucleus	BM	Left		*n.s*	14.54	$p_{FWE} < 1x10\text{-}12$		*n.s*		*n.s*
Medial amygdaloid nucleus	Me	Left		*n.s*	14.54	$p_{FWE} < 1x10\text{-}12$		*n.s*		*n.s*
Midbrain										
Midbrain	MD	Left	5.83	$p_{FWE} = 1.25x10\text{-}4$	8.32	$p_{FWE} < 1x10\text{-}12$		*n.s*		*n.s*
		Right		*n.s*	11.07	$p_{FWE} < 1x10\text{-}12$		*n.s*		*n.s*
Cerebellum										
Cerebellum	Cb	Left	8.38	$p_{FWE} < 1x10\text{-}12$	13.74	$p_{FWE} < 1x10\text{-}12$		*n.s*	7.53	$p_{FWE} = 2.29x10\text{-}9$
		Right	8.41	$p_{FWE} < 1x10\text{-}12$	14.03	$p_{FWE} < 1x10\text{-}12$		*n.s*	5.31	$p_{FWE} = 1.8x10\text{-}3$

Table S3: fMRI activations during low central thalamic (CT), high CT-DBS, low ventral-lateral thalamic (VL) and high VL-DBS

Thalamic DBS-induced fMRI activity during the electrical stimulation block-design experiment, $p < 0.05$, FWE corrected, ns: non significant.

Value	BF10	BF01
>100	Obvious evidence for H1	Obvious evidence for H0
30 to 100	Very strong evidence for H1	Very strong evidence for H0
10 to 30	Strong evidence for H1	Strong evidence for H0
3 to 10	Substantial evidence for H1	Substantial evidence for H0
1 to 3	Anecdotal evidence for H1	Anecdotal evidence for H0
1	No evidence for H1 or H0	
1 to 0.33	Anecdotal evidence for H0	Anecdotal evidence for H1
0.33 to 0.10	Substantial evidence for H0	Substantial evidence for H1
0.10 to 0.03	Strong evidence for H0	Strong evidence for H1
0.03 to 0.01	Very strong evidence for H0	Very strong evidence for H1
<0.01	Obvious evidence for H0	Obvious evidence for H1

Table S4: Interpretation of the Bayes Factors.

Value of the Bayes Factor BF10 and BF01 to interpret statistical evidence in favor of the H1 or H0 hypothesis. A BF greater than 3 significatively support the evidence of the tested hypothesis.

fMRI activations during the auditory "Local-Global" experiment

Local effect

Group

			Anesthesia		High CT-DBS		High CT-BS > Anesthesia	
Area	**Abbreviation**	**Hemisphere**	**T score**	**p value**	**T score**	**p value**	**T score**	**p value**
Orbitofrontal cortex								
Orbital Proisocortex	OPro	Left	4.44	$p_{FDR} = 0.047$		*n.s*		*n.s*
Parietal cortex								
Area 3b of cortex (somatosensory)	3b	Left	4.59	$p_{FDR} = 0.039$		*n.s*		*n.s*
Parietal area PG#1	PG#1	Right		*n.s*		*n.s*	4.24	$p_{FDR} = 0.044$
Visual area 4, Ventral part	V4V	Left		*n.s*	4.80	$p_{FDR} = 0.049$		*n.s*
Cingulate cortex								
Parietal area PE, Cingulate part	PECg	Left	4.80	$p_{FDR} = 0.037$		*n.s*		*n.s*
Temporal cortex								
Fundus of Superior Temporal sulcus	FST	Left	4.27	$p_{FDR} = 0.048$		*n.s*		*n.s*
ProKoniocortex, Medial part	ProKM	Left		*n.s*		*n.s*	4.59	$p_{FDR} = 0.040$
Temporal ParietoOccipital associated area in STS	TPO	Right		*n.s*		*n.s*	4.42	$p_{FDR} = 0.040$
Temporoparietal cortex	Tpt	Right		*n.s*		*n.s*	4.38	$p_{FDR} = 0.040$
Occipital cortex								
Visual area 1 (primary visual cortex)	V1	Left	4.41	$p_{FDR} = 0.047$		*n.s*		*n.s*
Striatum								
Caudate nucleus	Cd	Right	4.28	$p_{FDR} = 0.048$		*n.s*		*n.s*
Midbrain								
Midbrain	MB	Right		*n.s*		*n.s*	4.13	$p_{FDR} = 0.044$

Table S5: Cerebral activations for the local effect

fMRI activations for the local effect under anesthesia, high central thalamic (CT) DBS and comparison between high CT-DBS > anesthesia. Group results, $p < 0.05$, FDR corrected, ns: non significant.

fMRI activations during the auditory "Local-Global" experiment

Global effect

Group

			Awake		Anesthesia		High CT-DBS		High CT-DBS > Anesthesia	
Area	**Abbreviation**	**Hemisphere**	**Tscore**	**p value**	**Tscore**	**p value**	**Tscore**	**p value**	**Tscore**	**p value**
Frontal cortex										
Area 6 of the cortex, DorsoRostral part (Matellis F7)	6DR	Right		*n.s*		*n.s*	3.66	p_{FDR} =0.023		*n.s*
Area 6 of the cortex, Ventral part, Rostral subdivision (Matellis F5)	6VR	Left	3.88	p_{FDR} =*0.024*		*n.s*		*n.s*		*n.s*
Area 8B of cortex	8B	Right	4.61	p_{FDR} =*0.014*		*n.s*		*n.s*		*n.s*
Area 8B of cortex	9/46V	Right	3.82	p_{FDR} =*0.026*		*n.s*		*n.s*		*n.s*
Area 44 ofcortex	44	Right	3.58	p_{FDR} =*0.033*		*n.s*	4.75	p_{FDR} =*0.002*	4.57	p_{FDR} =*0.018*
				n.s		*n.s*	3.48	p_{FDR} =*0.031*		*n.s*
Area 45B of cortex	45B	Left	3.92	p_{FDR} =*0.024*		*n.s*	3.94	p_{FDR} =*0.014*		*n.s*
		Right		*n.s*		*n.s*		*n.s*	4.57	p_{FDR} =*0.018*
Area 47 (old 12) of cortex, Orbital part	47O	Left	3.91	p_{FDR} =*0.024*		*n.s*	3.83	p_{FDR} =*0.017*		*n.s*
		Right	4.09	p_{FDR} =*0.018*		*n.s*		*n.s*		*n.s*
Area ProM (promotor)	ProM#1	Left		*n.s*		*n.s*	3.80	p_{FDR} =*0.018*		*n.s*
Parietal cortex										
Area 3a of cortex (somatosensory)	3a	Right		*n.s*		*n.s*	5.06	p_{FDR} =*0.002*		*n.s*
				n.s		*n.s*	3.50	p_{FDR} =0.030		*n.s*
				n.s		*n.s*	3.47	p_{FDR} =0.031		*n.s*
Area 3b of cortex (somatosensory)	3b	Left			4.73	p_{FDR} =*0.042*		*n.s*		*n.s*
Parietal area PFG	PFG#1	Right	4.20	p_{FDR} =*0.017*		*n.s*		*n.s*	4.29	p_{FDR} =*0.018*
Depth IntraParietal area	DIP	Left		*n.s*		*n.s*		*n.s*	4.06	p_{FDR} =*0.028*
		Right		*n.s*		*n.s*	4.11	p_{FDR} =0.010		*n.s*
Parietal area PG	PG#1	Right	3.76	p_{FDR} =*0.028*		*n.s*	3.98	p_{FDR} =0.013		*n.s*
Dorsal parietal area	Dpt	Right		*n.s*		*n.s*	4.86	p_{FDR} =0.002		*n.s*
Parietal area Poa, external part	POaE	Left	3.39	p_{FDR} =*0.042*		*n.s*	4.51	p_{FDR} =0.005		*n.s*
Parietal area Poa, internal part	POaI	Left	3.56	p_{FDR} =*0.034*		*n.s*		*n.s*		*n.s*
Secondary somatosensory cortex	S2	Right		*n.s*		*n.s*	3.25	p_{FDR} =0.043		*n.s*
Secondary soamatosensory cortex, External part	S2E	Right		*n.s*		*n.s*	3.70	p_{FDR} =0.021		*n.s*
Visual area 4, Ventral part	V4V	Left		*n.s*		*n.s*	3.39	p_{FDR} =0.035	4.32	p_{FDR} =*0.018*
Visual area 4, Trnasitional part	V4T	left	4.37	p_{FDR} =*0.017*		*n.s*				*n.s*
Visual area 4, Dorsal part	V4D	Left		*n.s*		*n.s*	3.58	p_{FDR} =0.026		*n.s*
		Right		*n.s*		*n.s*	3.76	p_{FDR} =0.019		*n.s*
Cingulate cortex										
Area 23c of cortex	23c	Left		*n.s*		*n.s*	3.60	p_{FDR} =0.024		*n.s*
Area 24b of cortex	23b	Left	3.45	p_{FDR} =*0.039*		*n.s*		*n.s*		*n.s*
Temporal cortex										
Medial Superior Temporal area	MST	Left		*n.s*		*n.s*	3.24	p_{FDR} =*0.044*		*n.s*
		Right	4.05	p_{FDR} =*0.019*	4.46	p_{FDR} =*0.042*		*n.s*		*n.s*
Fundus of Superior Temporal sulcus	FST	Left		*n.s*		*n.s*	3.33	p_{FDR} =0.039		*n.s*
Superior Temporal sulcus area, gyral part	ST2g	Left		*n.s*		*n.s*	3.76	p_{FDR} =0.019		*n.s*
retroinsular area, Temporal part	RelT	Right	3.76	p_{FDR} =*0.028*		*n.s*		*n.s*		*n.s*
Temporal area TEa	TEa#1	Left	4.12	p_{FDR} =*0.018*		*n.s*	4.87	p_{FDR} =0.002	4.78	p_{FDR} =*0.018*
Temporal area TE, Occipital part	TEO	Left		*n.s*		*n.s*	3.27	p_{FDR} =0.042	4.32	p_{FDR} =*0.018*
Temporal ParietoOccipital associated area in STS	TPO	Left		*n.s*		*n.s*	5.37	p_{FDR} =0.002	4.62	p_{FDR} =*0.018*
				n.s		*n.s*		*n.s*	4.27	p_{FDR} =*0.018*
Occipital cortex										
Visual area 1 (primary visual cortex)	V1	Left			4.19	p_{FDR} =*0.042*		*n.s*		*n.s*
		Right			4.33	p_{FDR} =*0.042*	4.39	p_{FDR} =0.006		*n.s*
					4.30	p_{FDR} =*0.042*	3.90	p_{FDR} =0.015		*n.s*
Visual area 2	V2	Left				*n.s*	3.57	p_{FDR} =0.026		*n.s*
		Right	3.91	P_{FDR} =*0.024*	4.53	p_{FDR} =*0.042*	4.62	P_{FDR} =0.004		*n.s*
			3.58	P_{FDR} =*0.033*	4.46	p_{FDR} =*0.042*		*n.s*		*n.s*
Visual area 3, Ventral part	V3V	Right		*n.s*		*n.s*	4.27	p_{FDR} =0.007		*n.s*
				n.s		*n.s*	3.76	p_{FDR} =0.019		*n.s*
Visual area 3, Dorsal part	V3D	Right		*n.s*		*n.s*	3.88	p_{FDR} =*0.015*		*n.s*
Visual area 3A	V3A	Right		*n.s*		*n.s*	3.70	p_{FDR} =0.021		*n.s*

fMRI activations during the auditory "Local-Global" experiment

Global effect

Group

			Awake		Anesthesia		High CT-DBS		High CT-DBS > Anesthesia	
Area	**Abbreviation**	**Hemisphere**	**T score**	**p value**	**T score**	**p value**	**T score**	**p value**	**T score**	**p value**
Striatum										
Caudate nucleus	Cd	Right	4.61	p_{FDR} =0.014		*n.s*	4.83	p_{FDR} =0.002		*n.s*
Putamen	Pu	Right	4.66	p_{FDR} =0.007		*n.s*	4.27	p_{FDR} =0.007		*n.s*
				n.s		*n.s*	3.77	p_{FDR} =0.019		*n.s*
Thalamus										
Ventral PosteroLateral thalamic nucleus	VPL#1	Right			4.72	p_{FDR} =0.042		*n.s*		*n.s*
Ventral Anterior thalamic nucleus, Medial part	VAM	Left		*n.s*		*n.s*	3.66	p_{FDR} =0.023		*n.s*
MedioDorsalthalamic nucleus, Lateral part	MDL	Left		*n.s*		*n.s*		*n.s*	3.81	p_{FDR} =0.039
Reticular thalamic nucleus	R#4	Left		*n.s*		*n.s*		*n.s*	3.83	p_{FDR} =0.037
Lateral Geniculate Nucleus	LGN	Left		*n.s*		*n.s*	4.08	p_{FDR} =0.011		*n.s*
		Right		*n.s*		*n.s*	3.49	p_{FDR} =0.030		*n.s*
				n.s		*n.s*	3.45	p_{FDR} =0.033		*n.s*
Paraseptal subpallium										
Accumbens nucleus	Acb	Left		*n.s*		*n.s*		*n.s*	4.38	p_{FDR} =0.018
Midbrain										
Midbrain	MB	Right		*n.s*		*n.s*	4.43	p_{FDR} =0.006		*n.s*
Cerebellum										
Cerebellum	Cb	Left	4.83	p_{FDR} =0.014		*n.s*	3.32	p_{FDR} =0.039		*n.s*
		midline		*n.s*		*n.s*			4.21	p_{FDR} =0.020
		Right	3.57	p_{FDR} =0.033		*n.s*	3.65	p_{FDR} =0.023		*n.s*
				n.s		*n.s*	3.64	p_{FDR} =0.023		*n.s*

Table S6: Cerebral activations for the global effect

fMRI activations for the global effect in the awake, anesthesia and high central thalamic (CT) DBS condition and comparison between high CT-DBS versus anesthesia. For the global effect, no regions are significantly different for the awake > high CT-DBS comparison. Group results, $p < 0.05$, FDR corrected, ns: non significant.

Cerebral areas labelling using the CIVM macaque brain atlas Revised version

Level	Labels CIVM	Abbreviations CIVM	Value CIVM	Labels CIVM_R	Abbreviations CIVM_R	Value CIVM_R left	Value CIVM_R
						0	0
ventricles	ventricles	LV	1				
medulla	medulla	Md	2	MEDULLA	Md	1	2
pons	pons	Pn	3	PONS	Pn	3	4
cerebellum	cerebellum	Cb	4	CEREBELLUM	Cb	5	6
midbrain	midbrain	MB	5	MIDBRAIN	MB	7	8
thalamus	anterior pulvinar	Apul	6	PULVINAR	Pul	9	10
thalamus	anteromedial thalamic nucleus	AM#1	7	ANTERO THALAMIC NUCLEUS	A#1	11	12
thalamus	anteroventral thalamic nucleus	AV	8				
thalamus	central medial thalamic nucleus	CM#2	9	CENTRAL MEDIAL THALAMIC NUCLEUS	CM#2	13	14
thalamus	centrolateral thalamic nucleus	Cl#2	10	CENTROLATERAL THAKAMIC NUCLEUS	Cl#2	15	16
thalamus	centromedian thalamic nucleus, lateral part	CMnL	11	CENTROMEDIAN THALAMIC NUCLEUS	CMN	17	18
thalamus	centromedian thalamic nucleus, medial part	CMnM	12				
thalamus	inferior pulvinar	Ipul	13	PULVINAR	Pul	9	10
thalamus	interanteromedial thalamic nucleus	IAM	14	INTERANTEROMEDIAL THALAMIC NUCLEUS	IAM	19	20
thalamus	intermediodorsal thalamic nucleus	IMD	15	INTERMEDIODORSAL THALAMIC NUCLEUS	IMD	21	22
thalamus	lateral dorsal thalamic nucleus, superficial part	LDSF	16	LATERAL DORSAL THALAMIC NUCLEUS	LDSF	23	24
thalamus	lateral geniculate nucleus	LGN	17	LATERAL GENICULATE NUCLEUS	LGN	25	26
thalamus	lateral pulvinar	Lpul	18	PULVINAR	Pul	9	10
thalamus	medial geniculate nucleus, dorsal part	MGD	19				
thalamus	medial geniculate nucleus, medial part	MGM	20	MEDIAL GENICULATE NUCLEUS	MG	27	28
thalamus	medial geniculate nucleus, ventral part	MGV	21				
thalamus	medial pulvinar	MPul	22	PULVINAR	Pul	9	10
thalamus	mediodorsal thalamic nucleus, central part	MDC	23				
thalamus	mediodorsal thalamic nucleus, dorsal part	MDD	24	MEDIODORSAL THALAMIC NUCLEUS	MD	29	30
thalamus	mediodorsal thalamic nucleus, lateral part	MDL	25				
thalamus	mediodorsal thalamic nucleus, medial part	MDM	26				
thalamus	parafascicular thalamic nucleus	Pf#2	27	PARAFASCICULAR THALAMIC NUCLEUS	Pf#2	31	32
thalamus	paraventricular thalamic nucleus	PV	28	PARAVENTRICULAR THALAMIC NUCLEUS	PV	33	34
thalamus	paraventricular thalamus	PVT	29				
thalamus	pulvinar nuclei	Pul#1	30	PULVINAR	Pul	9	10
thalamus	reticular thalamic nucleus	R#4	31	RETICULAR THALAMIC NUCLEUS	R#4	35	36
thalamus	reuniens thalamic nucleus	Re	32			0	0
thalamus	suprageniculate thalamic nucleus	SG	33	SUPRAGENICULATE THALAMIC NUCLEUS	SG	37	38
thalamus	ventral anterior thalamic nucleus, lateral part, pallidal territory of thalamu	VAL(pal)	34				
thalamus	ventral anterior thalamic nucleus, lateral part, ventralis oralis nucleus	VAL(VO)	35	VENTRAL ANTERIOR THALAMIC NUCLEUS	VAL	39	40
thalamus	ventral anterior thalamic nucleus, magnocellular part	VAMC	36				
thalamus	ventral anterior thalamic nucleus, medial part	VAM	37				
thalamus	ventral lateral thalamic nucleus, lateral part	VLL	38	VENTRAL LATERAL THALAMIC NUCLEUS	VL	41	42
thalamus	ventral lateral thalamic nucleus, medial part	VLM#1	39				
thalamus	ventral posterolateral thalamic nucleus	VPL#1	40	VENTRAL POSTEROLATERAL THALAMIC NUCLEUS	VPL	43	44
thalamus	ventral posteromedial thalamic nucleus	VPM	41				
hypothalamus	hypothalamus	Hy	42	HYPOTHALAMUS	Hy	45	46
central subpallium	bed nucleus of the stria terminalis central division	BST	43			0	0
pallidum	external globus pallidus	EGP	44	EXTERNAL GLOBUS PALLIDUS	EGP	47	48
pallidum	internal globus pallidus	IGP	45	INTERNAL GLOBUS PALLIDUS	IGP	49	50
pallidum	ventral pallidum	VP#3	46	VENTRAL PADDIDUM	VP#3	51	52
paraseptal subpallium	accumbens nucleus, core	AcbC	47		Acb	53	54
paraseptal subpallium	accumbens nucleus, shell	AcbSh	48	ACCUMBENS NUCLEUS	Acb	53	54
paraseptal subpallium	accumbens nucleus	Acb	49		Acb	53	54
paraseptal subpallium	basal nucleus (Meynert)	BM#4	50	MEYNERT BASAL NUCLEUS	BM#4	55	56
paraseptal subpallium	nucleus of the horizontal limb of the diagonal band	HDB	51	UCLEUS OF HORIZONTAL LIMB OF DIAGONAL BAN	HDB	57	58
paraseptal subpallium	substantia innominata	SI	52			0	0
striatum	caudate nucleus	Cd	53	CAUDATE NUCLEUS	Cd	59	60
striatum	olfactory tubercle	Tu	54	OLFACTORY TUBERCLE	Tu	61	62
striatum	putamen	Pu	55	PUTAMEN	Pu	63	64
subpallial amygdala	amygdalohippocampal area	AHi	56				
subpallial amygdala	anterior amygdaloid area	AA	57				
subpallial amygdala	bed nucleus of the stria terminalis intraamygdaloid division	BSTIA	58	AMYGDALA	AMY	65	66
subpallial amygdala	central amygdaloid nucleus, lateral division	CeL	59				
subpallial amygdala	central amygdaloid nucleus, medial division	CEm#1	60				
subpallial septum	septum	Se	61			0	0
lateral pallium	dorsal endopiriform nucleus	DEn	62			0	0
ventral pallium	amygdalohippocampal area, magnocellular part	AHiMC	63				
ventral pallium	amygdalohippocampal area, parvicellular part	AHiPC	64				
ventral pallium	amygdalopiriform transition area	APir	65				
ventral pallium	anterior olfactory nucleus	AO	66				
ventral pallium	basolateral amygdaloid nucleus	BL#2	67				
ventral pallium	basolateral amygdaloid nucleus, dorsal part	BLD	68				
ventral pallium	basolateral amygdaloid nucleus, intermediate part	BLI	69				
ventral pallium	basolateral amygdaloid nucleus, ventral part	BLV	70				
ventral pallium	basolateral amygdaloid nucleus, ventrolateral part	BLVL	71				
ventral pallium	basolateral amygdaloid nucleus, ventromedial part	BLVM	72				
ventral pallium	basomedial amygdaloid nucleus	BM#3	73				
ventral pallium	lateral amygdaloid nucleus	La#3	74				
ventral pallium	medial amygdaloid nucleus	Me	75				
ventral pallium	paralaminar amygdaloid nucleus	PaL	76				
ventral pallium	piriform cortex	Pir	77				
ventral pallium	ventral cortical amygdaloid nucleus	VCo	78	AMYGDALA	AMY	65	66
hippocampus	hippocampus	Hip	79	HIPPOCAMPUS	Hip	67	68
medial pallium	parasubiculum	PaS	80				
medial pallium	presubiculum	PrS	81	SUBICULAR COMPLEX	PS	69	70
medial pallium	prosubiculum	ProS#2	82				
medial pallium	subiculum	S#1	83				
insular cortex	agranular insular cortex	AI	84				
insular cortex	dysgranular insular cortex	DI#2	85	INSULAR CORTEX	IC	71	72
insular cortex	granular insular cortex	GI	86				
insular cortex	insular proisocortex	IPro	87				
cingulate cortex	area 23 of cortex	23	88				
cingulate cortex	area 23a of cortex	23a	89				
cingulate cortex	area 23b of cortex	23b	90	AREA 23 OF CORTEX	23	73	74
cingulate cortex	area 23c of cortex	23c	91				
cingulate cortex	area 24/23a of cortex	24/23a	92				
cingulate cortex	area 24/23b of cortex	24/23b	93	AREA 24/23a OF CORTEX	24/23a	75	76
cingulate cortex	area 24/23c of cortex	24/23c	94				
cingulate cortex	area 24a of cortex	24a	95				
cingulate cortex	area 24b of cortex	24b	96				
cingulate cortex	area 24c of cortex	24c	97	AREA 24a OF CORTEX	24	77	78
cingulate cortex	area 24d of cortex	24d	98				
cingulate cortex	area 29a of cortex	29a	99				
cingulate cortex	area 29a-c of cortex	29a-c	100	AREA 29a OF CORTEX	29	79	80
cingulate cortex	area 29d of cortex	29d	101				
cingulate cortex	area 30 of cortex	30	102	AREA 30 OF CORTEX	30	81	82
cingulate cortex	area 31 of cortex	31	103	AREA 31 OF CORTEX	31	83	84
cingulate cortex	area 32 of cortex	32	104	AREA 32 OF CORTEX	32	85	86
cingulate cortex	area PGM/31 of cortex	PGM/31	105	AREA PGM/31 OF CORTEX	PGM/31	87	88
cingulate cortex	parietal area PE, cingulate part	PECg	106	PARIETAL AREA PE, cingulate part	PECg	89	90
cingulate cortex	unnamed region sections 102-114, called 23 more anteriorly	23x	107			0	0
occipital cortex	juxtastriate area	JxSt	108	JUXTASTRIATE AREA	JxSt	91	92
occipital cortex	prostriate area	ProST	109	PROSTRIATE AREA	ProST	93	94
occipital cortex	visual area 1 (primary visual cortex)	V1	110	VISUAL AREA 1	V1	95	96
occipital cortex	visual area 2	V2	111	VISUAL AREA 2	V2	97	98
occipital cortex	visual area 3, dorsal part	V3D	112				
occipital cortex	visual area 3, ventral part	V3V	113	VISUAL AREA 3	V3	99	100
occipital cortex	visual area 3A	V3A	114				
parietal cortex	area 1 of cortex (somatosensory)	1#1	115	AREA 1 OF CORTEX	1#1	101	102
parietal cortex	areas 2/1 of cortex (somatosensory)	39844	116	AREA 2/1 OF CORTEX	2#1	103	104
parietal cortex	area 2 of cortex (somatosensory)	2#1	117				
parietal cortex	area 2 of cortex, vestibular part	2Ve	118	AREA 2 OF CORTEX	2	105	106
parietal cortex	area 3a of cortex (somatosensory)	3a	119				
parietal cortex	area 3b of cortex (somatosensory)	3b	120	AREA 3a OF CORTEX	3	107	108
parietal cortex	depth intraparietal area	DIP	121	DEPTH INTRAPARIETAL AREA	DIP	109	110
parietal cortex	dorsal parietal area	Dpt	122	DORSAL PARIETAL AREA	Dpt	111	112
parietal cortex	occipitoparietal area	OPt	123	OCCIPITOPARIETAL AREA	OPt	113	114
parietal cortex	parietal area PE	PE#1	124				
parietal cortex	parietal area PE, caudal part	PEC	125	PARIETAL AREA PE	PE	115	116
parietal cortex	parietal area PEa	PEa	126				
parietal cortex	parietal area PF (cortex)	PFCx	127	PARIETAL AREA PF	PFCx	117	118
parietal cortex	parietal area PF, opercular part	PFOp	128				
parietal cortex	parietal area PFG	PFG#1	129	PARIETAL AREA PFG	PFG#1	119	120
parietal cortex	parietal area PG	PG#1	130	PARIETAL AREA PG	PG#1	121	122
parietal cortex	parietal area PG, opercular part	PGOp	131				
parietal cortex	parietal area POa, external part	POaE	132	PARIETAL AREA Poa	POa	123	124
parietal cortex	parietal area POa, internal part	POaI	133				
parietal cortex	parieto-occipital area	PO#1	134	PARIETO-OCCIPITAL AREA	PO#1	125	126
parietal cortex	parietooccipital associated area in the intraparietal sulcus	POa	135				
parietal cortex	posterior parietal area	PPt#1	136	POSTERIOR PARIETAL AREA	PPt#1	127	128
parietal cortex	retroinsular area, parietal part	ReIP	137	RETROINSULAR AREA, parietal part	ReIP	129	130
parietal cortex	secondary somatosensory cortex	S2	138				
parietal cortex	secondary somatosensory cortex, external part	S2E	139	SECONDARY SOMATOSENSORY CORTEX	S2	131	132
parietal cortex	secondary somatosensory cortex, internal part	S2I	140				
parietal cortex	visual area 4, dorsal part	V4D	141				
parietal cortex	visual area 4, transitional part	V4T	142	VISUAL AREA 4	V4	133	134
parietal cortex	visual area 4, ventral part	V4V	143				
parietal cortex	visual area 4A	V4A	144				

Cerebral areas labelling using the CIVM macaque brain atlas Revised version

Level	Labels CIVM	Abbreviations CIVM	Value CIVM	Labels CIVM_R	Abbreviations CIVM_R	Value CIVM_R left	Value CIVM_R
temporal cortex	area 35 of cortex	35	145	AREA 35 OF CORTEX	35	135	136
temporal cortex	area PG associated region of the superior temporal sulcus	PGa	146	REA PG, associated region of superior temporal sulc	PGa	137	138
temporal cortex	area TF, medial part	TFM	147	AREA TF, medial part	TFM	139	140
temporal cortex	area TL, rostral part (area 36R)	TLR(R36)	148	AREA TL, rostral part (area 36R)	TLR(R36)	141	142
temporal cortex	auditory koniocortex, lateral part	AKL	149	AUDITORY KONIOCORTEX	AK	143	144
temporal cortex	auditory koniocortex, medial part	AKM	150				
temporal cortex	entorhinal cortex, caudal limited part	ECL	151	ENTORHINAL CORTEX	ECL	145	146
temporal cortex	entorhinal cortex, caudal part	EC#2	152				
temporal cortex	entorhinal cortex, lateral part, caudal division	ELC	153				
temporal cortex	entorhinal cortex, lateral part, rostral division	ELR	154				
temporal cortex	entorhinal cortex, rostral part	ER#1	155				
temporal cortex	entorhinal Cx, intermediate part	EI	156				
temporal cortex	entorhinal Cx, olfactory part	EOl	157				
temporal cortex	fundus of superior temporal sulcus	FST	158	FUNDUS OF SUPERIOR TEMPORAL SULCUS	FST	147	148
temporal cortex	intraparietal sulcus associated area in the superior temporal sulcus	IPa	159	INTRAPARIETAL SULCUS ASSOCIATED AREA	IPa	149	150
temporal cortex	medial superior temporal area	MST	160	MEDIAL SUPERIOR TEMPORAL AREA	MST	151	152
temporal cortex	middle temporal area (visual area 5)	MT(V5)	161	MIDDLE TEMPORAL AREA (visual area 5)	MT(V5)	153	154
temporal cortex	paraauditory area, caudal part	PaAC	162	PARAAUDITORY CORTEX	PaA	155	156
temporal cortex	paraauditory area, lateral part	PaAL	163				
temporal cortex	paraauditory cortex, rostral part	PaAR	164				
temporal cortex	parainsular cortex, lateral part	PaIL	165	PARAINSULAR CORTEX	PaI	157	158
temporal cortex	parainsular cortex, medial part	PaIM	166				
temporal cortex	prokoniocortex	ProK	167	PROKONIOCORTEX	ProK	159	160
temporal cortex	prokoniocortex, lateral part	ProKL	168				
temporal cortex	prokoniocortex, medial part	ProKM	169				
temporal cortex	retroinsular area	ReI	170	RETROINSULAR AREA	ReI	161	162
temporal cortex	retroinsular area, temporal part	ReIT	171				
temporal cortex	superior temporal sulcus area 1	ST1	172	SUPERIOR TEMPORAL SULCUS	ST1	163	164
temporal cortex	superior temporal sulcus area 3	ST3	173				
temporal cortex	superior temporal sulcus area, gyral part	ST2g	174				
temporal cortex	superior temporal sulcus area, sulcal part	ST2s	175				
temporal cortex	temporal area TAa	TAa	176	TEMPORAL AREA TAa	TAa	165	166
temporal cortex	temporal area TE, medial part	TEM	177	TEMPORAL AREA TE	TE	167	168
temporal cortex	temporal area TE, occipital part	TEO	178				
temporal cortex	temporal area TE, occipitomedial part	TEOM	179				
temporal cortex	temporal area TE1	TE1#1	180				
temporal cortex	temporal area TE2	TE2#1	181				
temporal cortex	temporal area TE3	TE3#1	182				
temporal cortex	temporal area TEa	TEa#1	183				
temporal cortex	temporal area TF	TF	184	TEMPORAL AREA TF	TF	169	170
temporal cortex	temporal area TF, lateral part	TFL	185				
temporal cortex	temporal area TF, occipital part	TFO	186				
temporal cortex	temporal area TH	TH	187	TEMPORAL AREA TH	TH	171	172
temporal cortex	temporal area TH, occipital part	Tho	188				
temporal cortex	temporal area TL	TL	189	TEMPORAL AREA TL	TL	173	174
temporal cortex	temporal area TL, occipital part (area 36O)	TLO(36O)	190				
temporal cortex	temporal parietooccipital associated area in sts	TPO	191	TEMPORAL PARIETOOCCIPITAL ASSOCIATED AREA	TPO	175	176
temporal cortex	temporal parietooccipital associated area in sts, caudal part	TPOC	192				
temporal cortex	temporoparietal cortex	Tpt	193	TEMPOROPARIETAL CORTEX	Tpt	177	178
temporal cortex	temporopolar periallocortex	TTPAl	194	TEMPOROPOLAR PERIALLOCORTEX	TTPAl	179	180
temporal cortex	temporopolar proisocortex	TPPro	195	TEMPOROPOLAR PROISOCORTEX	TPPro	181	182
frontal cortex	area 4 of cortex (primary motor)	4#1	196	AREA 4 OF CORTEX (primary motor)	4#1	183	184
frontal cortex	area 6 of cortex, dorsocaudal part (Matellis F2)	6DC(F2)	197	AREA 6 OF CORTEX	6	185	186
frontal cortex	area 6 of cortex, dorsorostral part (Matellis F7)	6DR(F7)	198				
frontal cortex	area 6 of cortex, medial (supplementary motor) part	6M	199				
frontal cortex	area 6 of cortex, ventral part, caudal subdivision (Matellis F4)	6VC(F4)	200				
frontal cortex	area 6 of cortex, ventral part, rostral subdivision (Matellis F5)	6VR(F5)	201				
frontal cortex	area 6/32 of cortex	10379	202	AREA 6/32 OF CORTEX	6/32	187	188
frontal cortex	area 8 of cortex, anterodorsal part	8AD	203	AREA 8 OF CORTEX	8	189	190
frontal cortex	area 8 of cortex, anteroventral part	8AV	204				
frontal cortex	area 8/32 of cortex	10440	205				
frontal cortex	area 8A of cortex	8A	206				
frontal cortex	area 8B of cortex	8B	207				
frontal cortex	area 9 of cortex, lateral part	9L	208	AREA 9 OF CORTEX	9	191	192
frontal cortex	area 9 of cortex, medial part	9M	209				
frontal cortex	area 9/32 of cortex	10471	210	AREA 9/32 OF CORTEX	9/32	193	194
frontal cortex	area 9/46 of cortex	15584	211	AREA 9/46 OF CORTEX	9/46	195	196
frontal cortex	area 9/46 of cortex, dorsal part	9/46D	212				
frontal cortex	area 9/46 of cortex, ventral part	9/46V	213				
frontal cortex	area 10 of cortex	10	214	AREA 10 OF CORTEX	10	197	198
frontal cortex	area 10 of cortex, dorsal part	10D	215				
frontal cortex	area 10 of cortex, medial part	10M	216				
frontal cortex	area 10 of cortex, ventral part	10V	217				
frontal cortex	area 44 of cortex	44	218	AREA 44 OF CORTEX	44	199	200
frontal cortex	area 45A of cortex	45A	219	AREA 45 OF CORTEX	45	201	202
frontal cortex	area 45B of cortex	45B	220				
frontal cortex	area 46D of cortex	46D	221	AREA 46 OF CORTEX	46	203	204
frontal cortex	area 46V of cortex	46V	222				
frontal cortex	area 47 (old 12) of cortex	47(12)	223	AREA 47 OF CORTEX	47	205	206
frontal cortex	area 47 (old 12) of cortex, lateral part	47(12)L	224				
frontal cortex	area 47 (old 12) of cortex, orbital part	47(12)O	225				
frontal cortex	area ProM (promotor)	proM#1	226	AREA PROM (promotor)	proM#1	207	208
frontal cortex	gustatory cortex	Gu	227	GUSTATORY CORTEX	Gu	209	210
orbitofrontal cortex	area 11 of cortex	11	228	AREA 11 OF CORTEX	11	211	212
orbitofrontal cortex	area 11 of cortex, lateral part	11L	229				
orbitofrontal cortex	area 11 of cortex, medial part	11m	230				
orbitofrontal cortex	area 13 of cortex	13	231	AREA 13 OF CORTEX	13	213	214
orbitofrontal cortex	area 13 of cortex, lateral part	13L	232				
orbitofrontal cortex	area 13 of cortex, medial part	13M	233				
orbitofrontal cortex	area 13a of cortex	13a	234				
orbitofrontal cortex	area 14 of cortex, medial part	14M	235	AREA 14 OF CORTEX	14	215	216
orbitofrontal cortex	area 14o	14o	236				
orbitofrontal cortex	area 25 of cortex	25	237	AREA 25 OF CORTEX	25	217	218
orbitofrontal cortex	orbital periallocortex	OPAl	238	ORBITAL PERIALLOCORTEX	OPAl	219	220
orbitofrontal cortex	orbital proisocortex	OPro	239	ORBITAL PROISOCORTEX	OPro	221	222
white matter	cerebral white matter	cwm	240			0	0
white matter	external medullary lamina	eml	241			0	0

<u>Table S7</u>: Whole brain areas labelling of the Center for In Vivo Microscopy atlas (CIVM) atlas Revised (CIVM_R) for functional correlations analysis.

Whole brain regions considered for the functional correlations analysis using the macaque CIVM atlas*(76)* that was revised into CIVM_R to match fMRI spatial resolution. Regions merged together (for instance dorsal, medial and ventral part of the medial geniculate nucleus in the original CIVM atlas into medial geniculate nucleus) share the same abbreviation and value in the CIVM_R. Brackets represent the biggest regions unified. Empty cells stands for deleted regions.